Supplementary Methods

Mitochondrial Genome Assembly and Annotation.

To obtain the high-quality mitochondrial genome assemblies, the data from the long reads were used to de novo assemble the mitochondrial genome separately. The average coverage of previously published reads was downsampled to ~4 Gb. The mitochondrial genome assembly was constructed in SPAdes v.3.12.0 (1) and BLAST v.2.9.0 (2). First, the long and short reads (for each sample) were combined to assemble the draft mitochondrial contigs in the HYBRIDSPADES program integrated in SPAdes with the parameter "-k 127 -t 20 -m 500" followed Gu et al. (3). Second, the assembled contigs were aligned to the two previously published mitochondrial genomes from mandarin G1 or pummelo HBP in BLASTN with the parameter "-evalue 1e-6 -outfmt 6." As a result, the potential high-coverage mitochondrial contigs were filtered (length >5 kb, identity >95%). To further reduce the bias from the chloroplast and nuclear genomes, we filtered the contigs based on coverage estimations. Based on our data, the coverage of the chloroplast contigs was about three to five times higher than that of the mitochondrial sequences, and the coverage of the nuclear genome contigs was ~1/40 of the mitochondrial contigs. Subsequently, we aligned the assemblies to both the mitochondrial genomes of mandarin G1 and pummelo HBP. The results were combined to determine the order of the contigs. Notably, the assembly of the grapefruit cultivar JW was different because the mitochondrial sequences were directly obtained from the Illumina sequencing platform. Therefore, the assemblies for grapefruit cultivar JW were used only as short reads. The other steps were identical to the steps used with samples that were analyzed with both long and short reads. To increase the quality and continuity of each assembly, we performed Sanger sequencing to verify the linkage of contigs and to fill the gaps (*SI Appendix*, Table 3). Finally, two mitochondrial genome assemblies (three gaps in SJG

and two gaps in ZK) were assembled into circular physical maps. We collected the 10 contig-level assemblies and aligned them to the mitochondrial reference genome SJG in RaGOO v1.1 with the default options (4). As a result, we obtained 10 reference-guided scaffold-level assemblies. The gaps between the contigs were connected by “N.” The pan-genome of the mitochondrial genome in citrus was constructed in minigraph-0.13 (r397) with an incremental graph generation mode (https://github.com/lh3/minigraph). For the annotation of mitochondrial genomes, we used the MITOFY webserver to predict the conserved protein-coding genes (5). The ORFs were predicted in Unipro UGENE (v37.0) (6). Subsequently, we excavated the chimeric ORFs (>300 bp) containing conserved gene fragments in the intergenic region by using custom scripts (*SI Appendix*, Table 4). At the same time, the tRNA and ribosomal RNA genes were identified in tRNAscan-SE v1.21 and the RNAmmer 1.2 server with default parameters, respectively (7, 8).

Identification of Structural Variations.

To construct the mitochondrial SV maps, we identified four categories of SVs—deletions (DELs), insertions (INSs), inversions (INVs), and duplications (DUPs)—from three methods. First, we performed a whole-genome alignment by using MUM&Co with a genome size “-g 500000” (9), based on the kumquat SJG reference mitochondrial genome (filling the gaps). Second, we aligned the long reads from 11 citrus accessions to the kumquat SJG mitochondrial reference genome. Third, SVs were identified from Illumina short reads from 184 citrus accessions. When identifying the SVs from long read mapping, we mapped the PacBio/Nanopore long reads to the kumquat SJG reference mitochondrial genome in Minimap2 (10). The PacBio genomic reads were mapped in “-ax map-pb” mode, and Oxford Nanopore genomic reads were mapped in “-ax map-ont” mode. Then, the SVs were identified in Sniffles v2.0.6, followed by multiple-sample SV calling mode and cuteSV v1.0.13 with

the default options with different sequencing platforms (11, 12). For the SVs identified with Illumina short reads, we first trimmed the adapter sequences by using Fastp (13) and then mapped the clean reads to the kumquat SJG reference mitochondrial genome via Burrows–Wheeler alignment maximal exact match (14). SV site calling (BCF files) was based on BAM files in DELLY v1.0.3 followed by germline SV callingAQ11 mode (15). Subsequently, we used BCFtools to generate a VCF file including the SV genotypes. Finally, we plotted the BAM files by using the Integrative Genomics Viewer (IGV) v2.13.2 (16) and examined the split or link reads and the coverage depth for the SVs that we identified.

Construction of Variant Maps.

To elucidate the evolutionary patterns between cytoplasmic genomes and nuclear genomes, we generated three variation maps including the nuclear, mitochondrial, and chloroplast variation maps. The nuclear variation map was constructed with short reads from 184 accessions. The reads were mapped to the *Fortunella* reference nuclear genome (a chromosome-level reference) via Burrows–Wheeler alignment maximal exact match, after the removal of adapters in Fastp. The BAM alignment files were sorted with SAMtools (17). PCR duplicates were removed with MarkDuplicates in Picard 2.19.0 (https://github.com/broadinstitute/picard). The genotype information was obtained with Deepvariant (rc1.0.0) and default options (18). The GVCF filesAQ12 from 184 accessions were consolidated into a single VCF file in GLnexus (v1.2.7) with the DeepVariantWGS config (19). To obtain reliable population structure and robust phylogeny, we filtered nuclear genomic variations based on depth of coverage and missing rate. The SNPs and indels were filtered via VCFtools with the following criteria: variant quality >2.0, quality score >40.0, mapping quality >30.0, genotype calls with a depth >2 or <100, and <20% missing genotypes across all samples. In addition, the

nuclear variation dataset was pruned with LD values (10-kb sliding windows and an r^2 threshold of 0.5) for the phylogeny and population structure analysis.

The mitochondrial and chloroplast variation maps were also filtered with a depth >2 but were processed differently than the nuclear genomic sequence data in two aspects (1): homologous regions of the nuclear genome and (2) missing rate filtering. In detail, the regions of homology among the nuclear, mitochondrial, and chloroplast genomes were detected in BLASTN v.2.9.0, and the cytoplasmic genome variations in the homologous regions were marked. We observed low coverage in species-specific SVs that occurred because of occasional paternal leakage. Therefore, unfiltered mitochondrial and chloroplast variation maps were used to construct phylogenetic network trees and to estimate the level of mitochondrial heteroplasmy.

References

1. A. Bankevich *et al.*, SPAdes: A new genome assembly algorithm and its applications to single-cell sequencing. *J. Comput. Biol.* **19**, 455–477 (2012).

2. C. Camacho *et al.*, BLAST+: Architecture and applications. *BMC Bioinformatics* **10**, 421 (2009).

3. Z. Gu *et al.*, Cytoplasmic and nuclear genome variations of rice hybrids and their parents inform the trajectory and strategy of hybrid rice breeding. *Mol. Plant* **14**, 2056–2071 (2021).

4. M. Alonge *et al.*, RaGOO: Fast and accurate reference-guided scaffolding of draft genomes. *Genome Biol.* **20**, 224 (2019).

5. A. J. Alverson *et al.*, Insights into the evolution of mitochondrial genome size from complete sequences of *Citrullus lanatus* and *Cucurbita pepo* (Cucurbitaceae). *Mol. Biol. Evol.* **27**, 1436–1448 (2010).

6. R. Rose, O. Golosova, D. Sukhomlinov, A. Tiunov, M. Prosperi, Flexible design of multiple metagenomics classification pipelines with UGENE. *Bioinformatics* **35**, 1963–1965 (2019).

7. T. M. Lowe, S. R. Eddy, tRNAscan-SE: A program for improved detection of transfer RNA genes in genomic sequence. *Nucleic Acids Res.* **25**, 955–964 (1997).

8. K. Lagesen *et al.*, RNAmmer: Consistent and rapid annotation of ribosomal RNA genes. *Nucleic Acids Res.* **35**, 3100–3108 (2007).

9. S. O'Donnell, G. Fischer, MUM&Co: Accurate detection of all SV types through whole-genome alignment. *Bioinformatics* **36**, 3242–3243 (2020).

10. H. Li, Minimap2: Pairwise alignment for nucleotide sequences. *Bioinformatics* **34**, 3094–3100 (2018).

11. F. J. Sedlazeck *et al.*, Accurate detection of complex structural variations using single-molecule sequencing. *Nat. Methods* **15**, 461–468 (2018).

12. T. Jiang *et al.*, Long-read-based human genomic structural variation detection with cuteSV. *Genome Biol.* **21**, 189 (2020).

13. S. Chen, Y. Zhou, Y. Chen, J. Gu, fastp: An ultra-fast all-in-one FASTQ preprocessor. *Bioinformatics* **34**, i884–i890 (2018).

14. H. Li, Aligning sequence reads, clone sequences and assembly contigs with BWA-MEM. *arXiv: Genomics* (2013). https://doi.org/10.48550/arXiv.1303.3997.

15. T. Rausch *et al.*, DELLY: Structural variant discovery by integrated paired-end and split-read analysis. *Bioinformatics* **28**, i333–i339 (2012).

16. J. T. Robinson *et al.*, Integrative genomics viewer. *Nat. Biotechnol.* **29**, 24–26 (2011).

17. H. Li *et al.*; 1000 Genome Project Data Processing Subgroup, The sequence alignment/map format and SAMtools. *Bioinformatics* **25**, 2078–2079 (2009).

18. R. Poplin *et al.*, A universal SNP and small-indel variant caller using deep neural networks. *Nat. Biotechnol.* **36**, 983–987 (2018).

19. T. Yun *et al.*, Accurate, scalable cohort variant calls using DeepVariant and GLnexus. *Bioinformatics* **36**, 5582–5589 (2021).

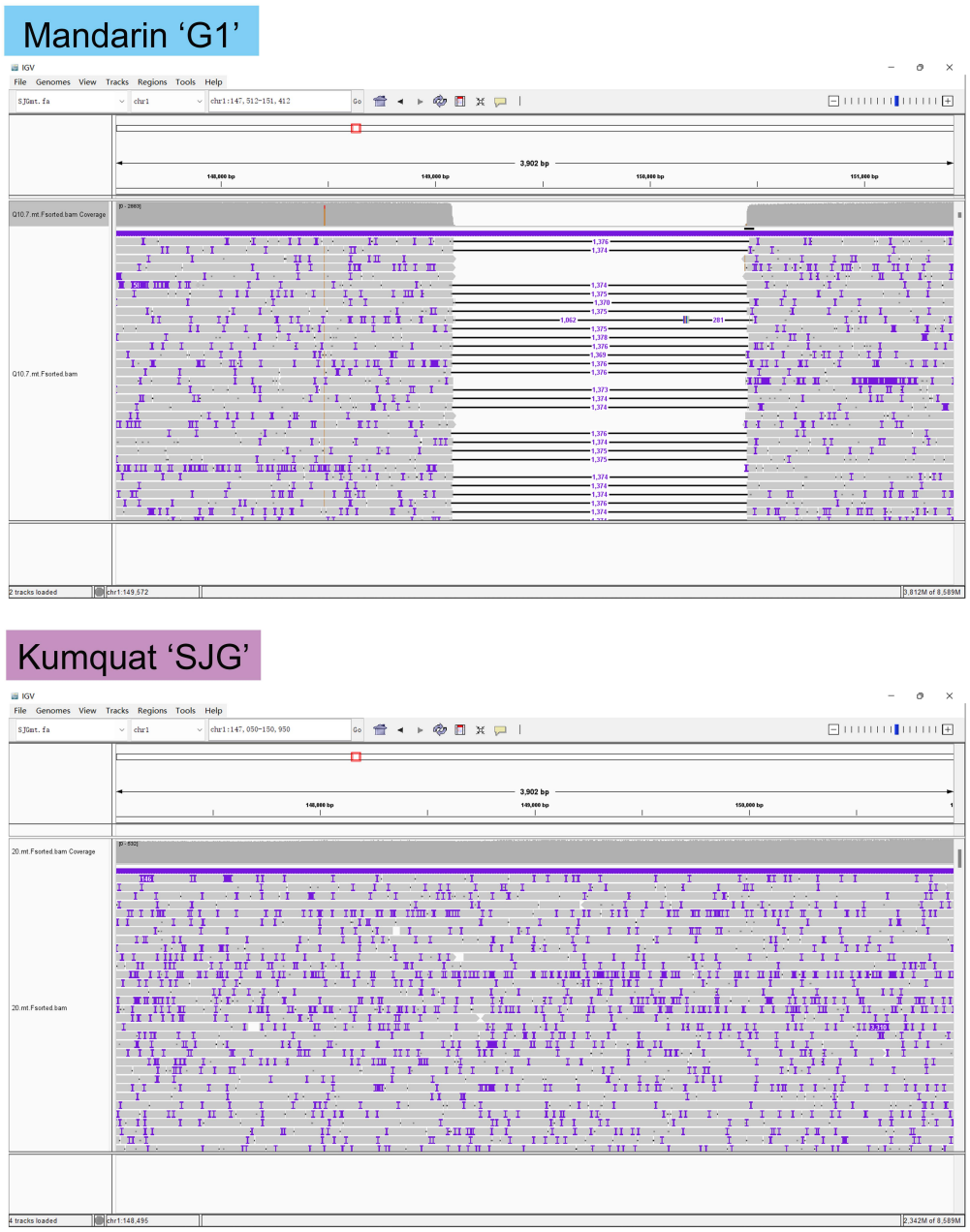

Supplementary Fig. 1. The example of 1375 bp deletion in mandarin G1 mitochondrial genome identified by the long-reads alignment. (A) The PacBio long reads from mandarin cultivar G1 were mapped to the kumquat SJG reference mitochondrial genome. (B) The PacBio long reads from kumquat SJG were mapped to its own mitochondrial genome. The window from 147,050 to150,950 bp.

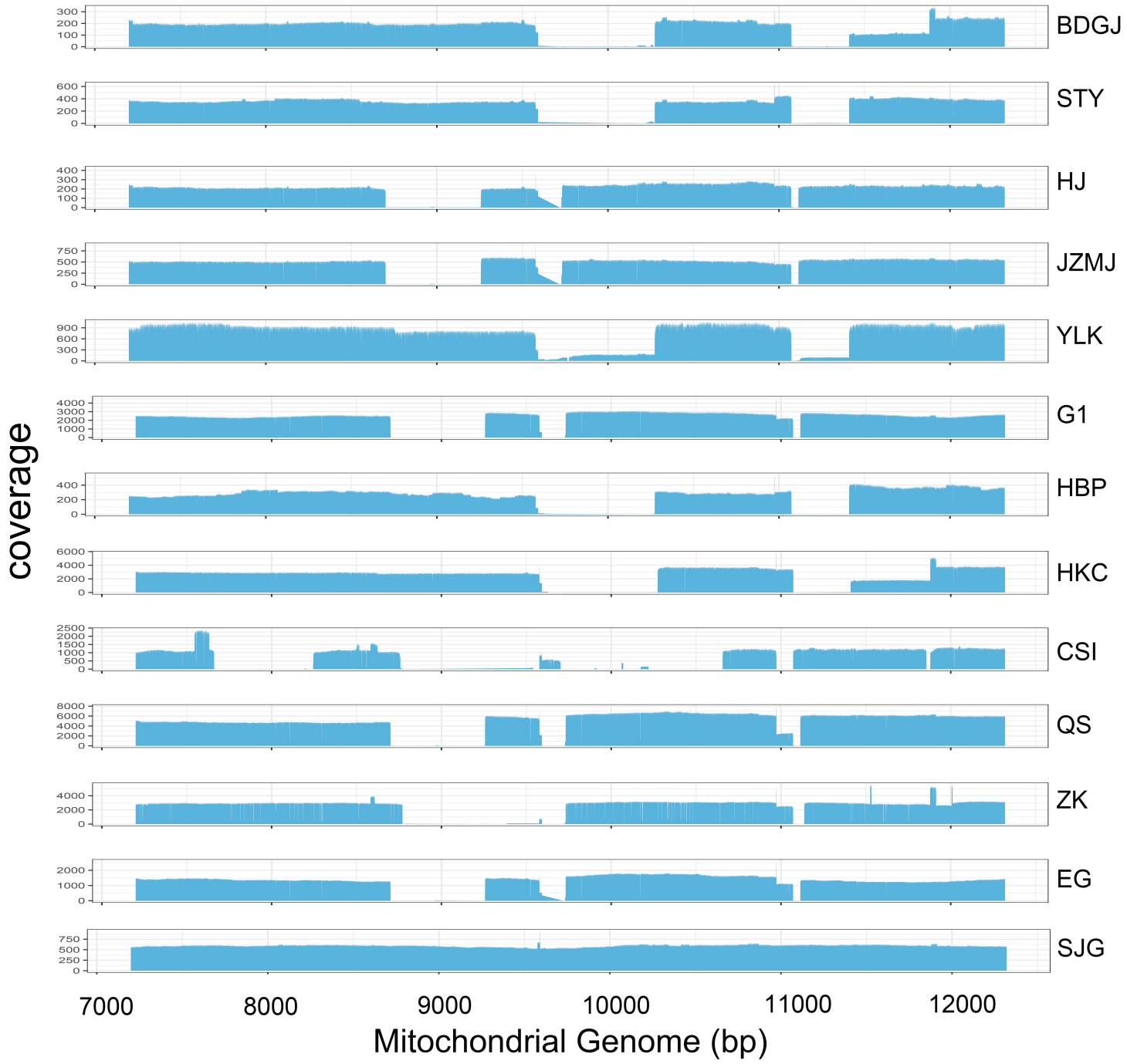

Supplementary Fig. 2. The SVs and coverage of long reads mapping in mitochondrial genome. The 13 accessions of PacBio or Nanopore long reads were mapped to the kumquat SJG reference mitochondrial genome. The x-axis showed the window from 7,000 to 12,000 bp. The y-axis showed the coverage of each accession.

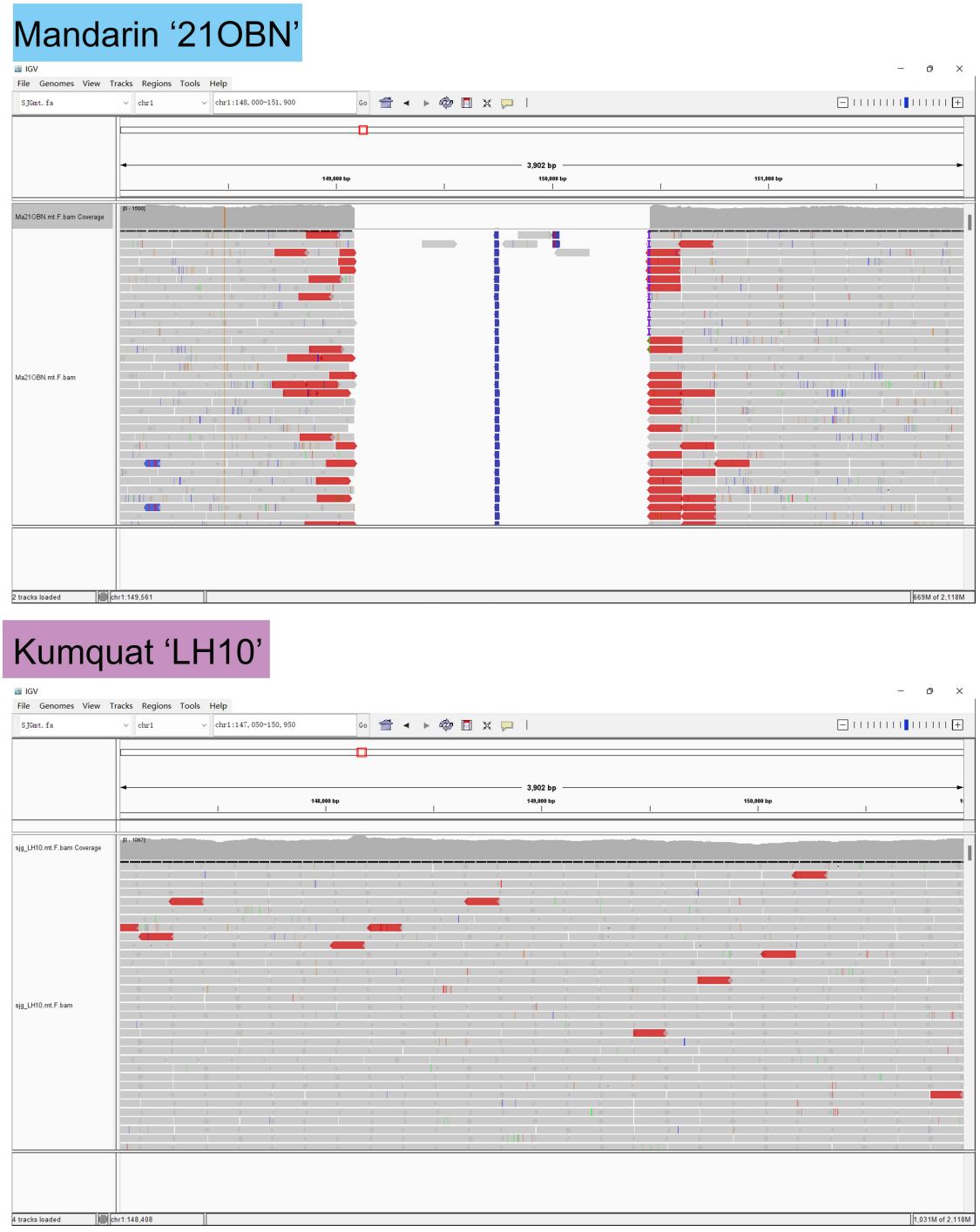

Supplementary Fig. 3. The example of 1375 bp deletion in mandarin ‘G1’ mitochondrial genome identified by the short-reads alignment. (A) The Illumina short reads from mandarin sequenced sample 21OBN were mapped to the kumquat SJG reference mitochondrial genome. (B) The Illumina short reads from kumquat sequenced sample LH10 were mapped to the kumquat SJG reference mitochondrial genome. The window from 147,050 to 150,950 bp as well as Supplementary Fig. 4.

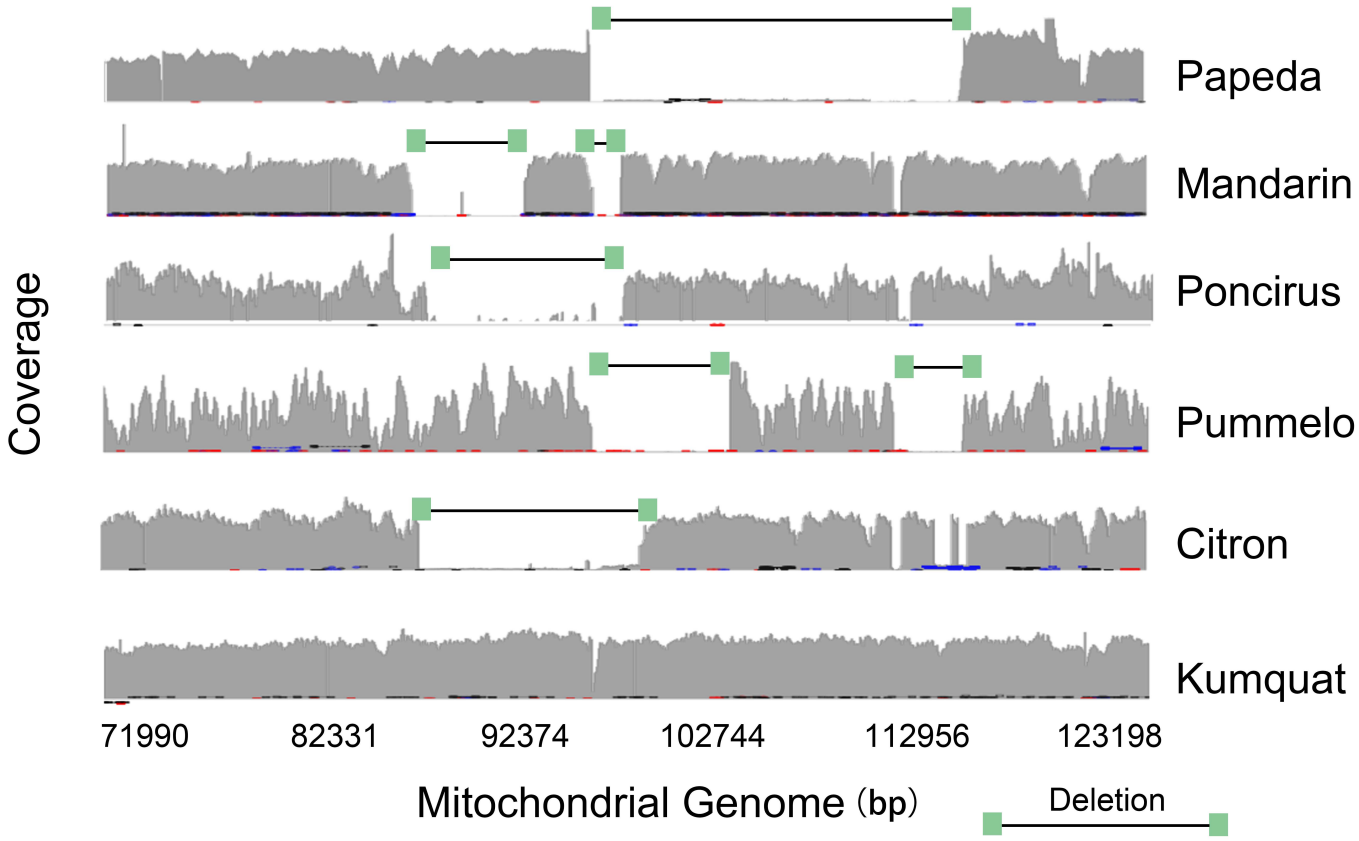

Supplementary Fig. 4. The SVs and coverage of short reads mapping in mitochondrial genome. The Illumina short reads in six individuals from six species (papeda, mandarin, poncirus, pummelo, citron and kumquat) were mapped to the kumquat SJG reference mitochondrial genome. The x-axis showed the window from 71,990 to 123,198 bp. The y-axis showed the coverage of each accession.

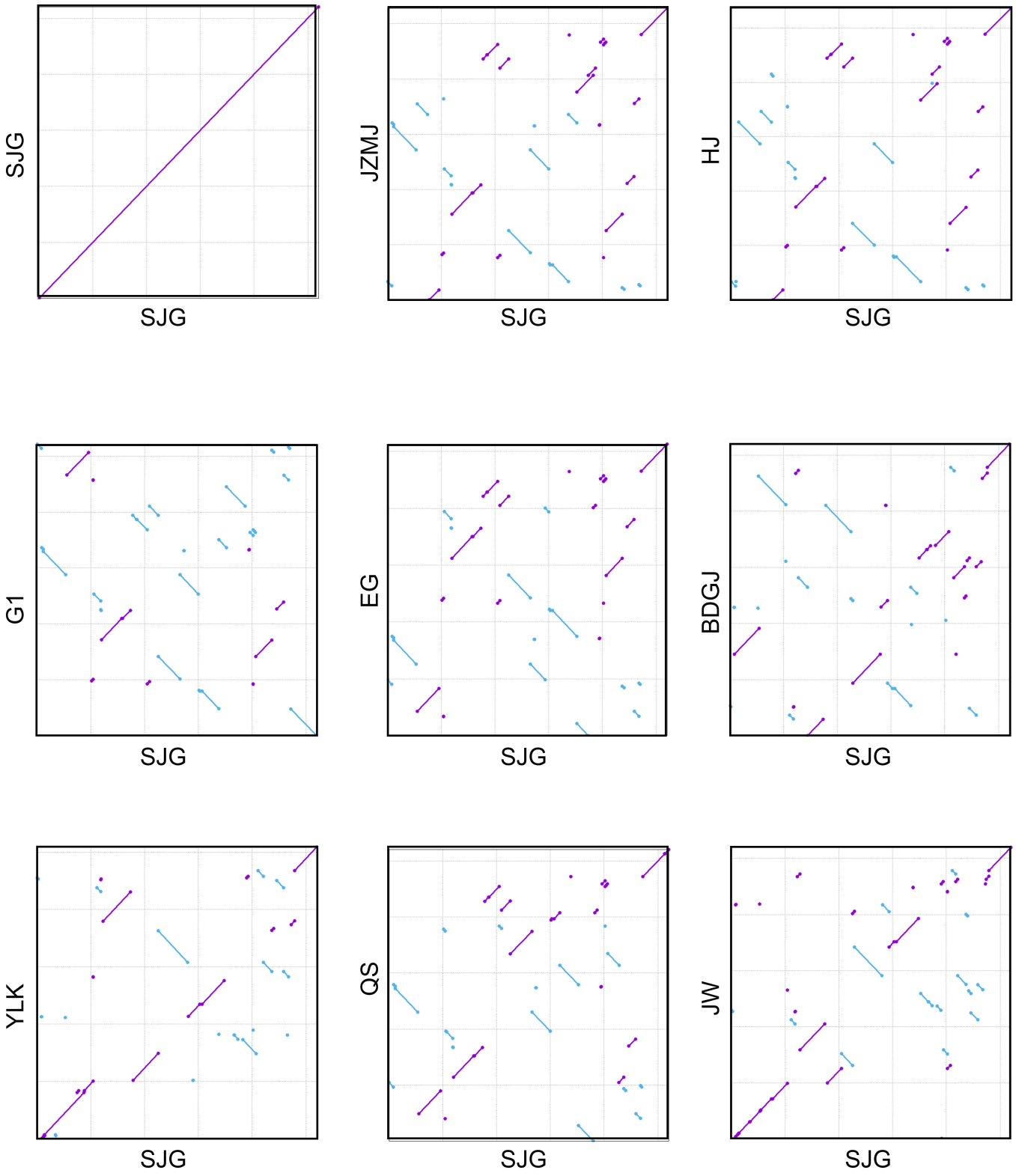

Supplementary Fig. 5. The collinearity analysis between nine assemblies and the kumquat SJG reference mitochondrial genome. The nine assemblies were linearized and mapped to the kumquat SJG reference mitochondrial genome. The x-axis showed the SJG mitochondrial genome, while the y-axis showed the nine target assemblies including the SJG mitochondrial genome.

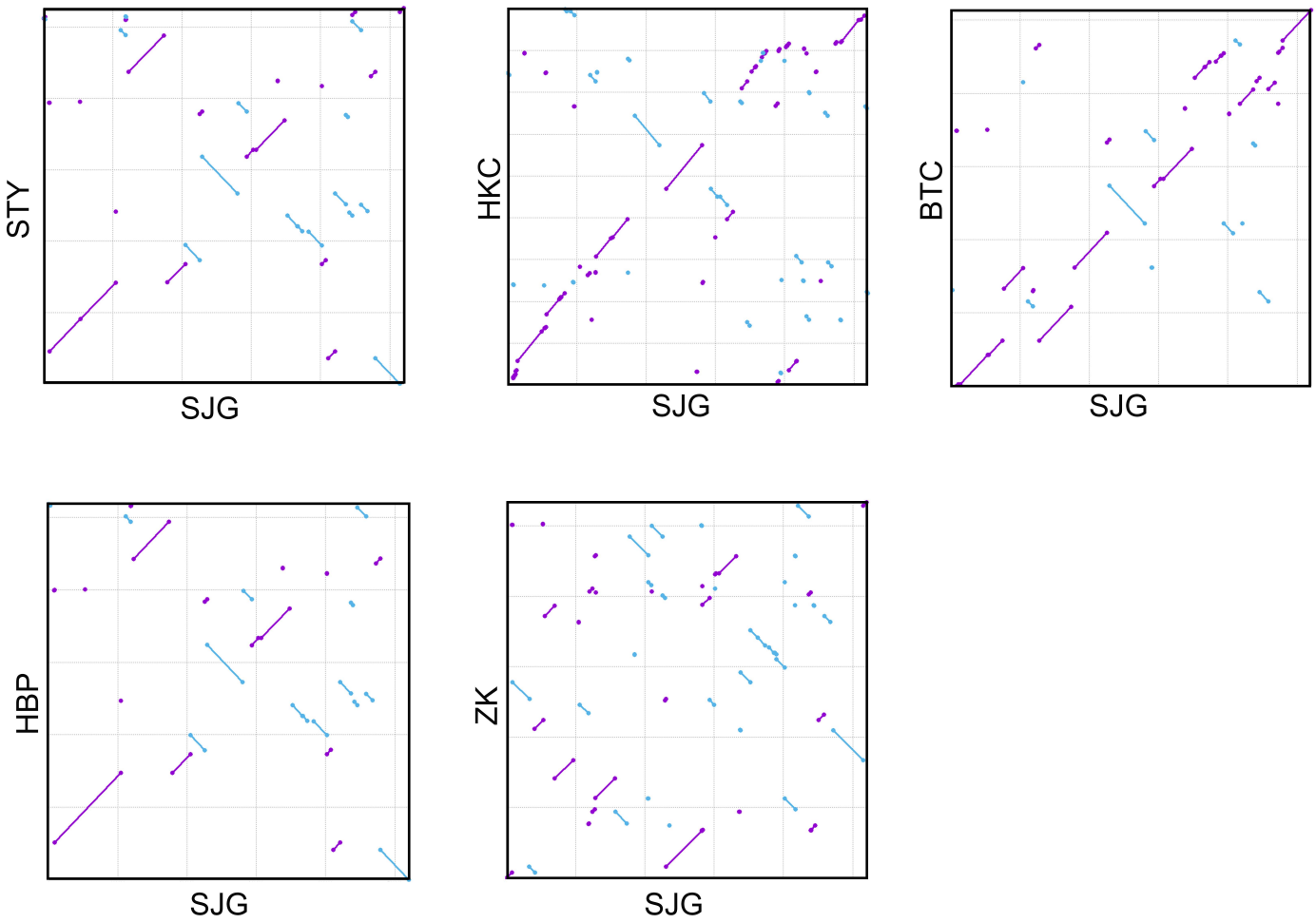

Supplementary Fig. 6. The collinearity analysis between five assemblies and the kumquat SJG reference mitochondrial genome. Five other assemblies added after the Supplementary Fig. 5.

A

B

HKC	1, 2, 3, 4, 5, 6, 7, 8, 9, 10, 11, 12, 13, 14, 15, 16, 17, 18, 19, 20, 21, 22, 23, 24, 25, 26, 27, 28, 29, 30, 31, 32, 33, 34, 35, 36, 37, 38, 39, 40, 41, 42, 43, 44, 45, 46, 47, 48, 49, 50, 51, 52, 53, 54, 55, 56, 57
ZK	14, 39, −22, −17, 51, 52, −10, −43, 15, −35, −37, −23, −28, −27, 29, 30, −36, 46, 47, 42, −11, −38, −21, 50, −49, 44, −8, 1, 5, −32, −31, 18, −16, −7, −40, 54, −9, 55, 56, 57, −13, −12, −25, −24, 53, 2, 3, 4, −20, 45, 41, 26, −19, −34, −33, 6, 48
SJG	1, 5, 6, 7, 11, 12, 13, −57, 18, −47, −46, −45, 20, 23, 24, 25, 26, −19, −37, −36, −35, −3, 32, 33, 34, 15, −42, −31, −30, −29, 27, 28, −41, −40, 44, −8, 50, −49, 53, 2, 4, −22, −17, 51, 52, −10, −43, 16, −38, −21, 54, −9, 55, 56, −39, −14, −48
HBP	−48, 16, 18, 19, −26, −25, −24, −23, −20, 45, 46, −54, 15, −42, 8, −44, 40, 41, −28, −27, 29, 30, 31, 32, 33, 34, −22, −17, 51, 52, −10, −43, −47, −38, −21, 50, −49, −36, −35, −3, −2, −53, 37, 57, −13, −12, −11, −7, −6, −5, −1, −4, −9, 55, 56, −39, −14
STY	14, 39, −56, −48, 16, 18, 19, −26, −25, −24, −23, −20, 45, 46, −54, 15, −42, 8, −44, 40, 41, −28, −27, 29, 30, 31, 32, 33, 34, −22, −17, 51, 52, −10, −43, −47, −38, −21, 50, −49, −36, −35, −3, −2, −53, 37, 57, −13, −12, −11, −7, −6, −5, −1, −4, −9, 55
BTC	1, 5, 6, 7, 11, 12, 23, 24, 25, 26, −19, −18, −16, 48, 13, −57, −37, −36, −35, −3, −2, −53, 49, −34, −33, −32, −31, −30, −29, 27, 28, −41, −40, 44, −8, 42, −15, −22, −17, 51, 52, −10, −43, −47, −38, −21, 50, 54, −46, −45, 20, −4, −9, 55, 56, −39, −14
JW	1, 5, 6, 7, 11, 12, 13, −57, −37, 53, 2, 3, 35, 36, 49, 23, 24, 25, 26, −19, −18, −16, 48, −50, 21, 38, 47, 43, 10, −52, −51, 17, 22, −34, −33, −32, −31, −30, −29, 27, 28, −41, −40, 44, −8, 42, −15, 54, −46, −45, 20, −4, −9, 55, 56, −39, −14
YLK	1, 5, 6, 7, 11, 12, 13, −57, −37, −36, −35, −3, −2, −53, 49, −50, 15, −42, −31, −30, −29, 27, 28, −41, −40, 44, −8, 21, 38, 47, 43, 10, −52, −51, 17, 22, −34, −33, −32, 54, −46, −45, 20, 23, 24, 25, 26, −19, −18, −16, 48, −4, −9, 55, 56, −39, −14
BDGJ	25, 26, −19, −18, −16, 48, 41, −28, −27, 29, 30, 31, 32, 33, 34, 1, 5, 6, 7, 15, −42, 8, −44, 40, −24, −23, −22, −17, 51, 52, −10, −43, −47, −38, −21, 50, −49, 53, 2, 3, 35, 36, 37, 57, −13, −12, −11, 54, −46, −45, 20, −4, −9, 55, 56, −39, −14
EG	−50, 21, 38, 11, 12, 13, −57, 48, 42, −15, −34, −7, −6, −5, −1, 8, −44, 40, 41, −28, −27, 29, 30, −36, −33, −32, 3, 4, −22, −17, 51, 52, −10, −43, −47, −46, −45, 20, 23, 24, 25, 26, −19, 16, −18, 31, −35, −37, 53, 2, −49, 54, −9, 55, 56, −39, −14
G1	−48, 57, −13, −12, −11, −38, −21, 50, −35, −37, 53, 2, −49, 44, −8, 1, 5, 6, 7, 34, 15, −42, −31, 18, −16, 19, −26, −25, −24, −23, −20, 45, 46, 47, 43, 10, −52, −51, 17, 22, −4, −3, 32, 33, 36, −30, −29, 27, 28, −41, −40, 54, −9, 55, 56, −39, −14
HJ	13, −57, 48, −1, 8, −44, 40, 41, −28, −27, 29, 30, −36, −33, −32, 3, 4, −22, −17, 51, 52, −10, −43, −47, −46, −45, 20, 23, 24, 25, 26, −19, 16, −18, 31, 42, −15, −34, −7, −6, −5, −12, −11, −38, −21, 50, −35, −37, 53, 2, −49, 54, −9, 55, 56, −39, −14
JZMJ	13, −57, 48, 41, −28, −27, 29, 30, −36, −33, −32, 3, 4, −22, −17, 51, 52, −10, −43, −47, −46, −45, 20, 23, 24, 25, 26, −19, 16, −18, 31, 42, −15, −34, −7, −6, −5, −1, 8, −44, 40, −12, −11, −38, −21, 50, −35, −37, 53, 2, −49, 54, −9, 55, 56, −39, −14
QS	−50, 21, 38, 11, 12, 13, −57, 48, 52, −10, −43, −47, −46, −45, 20, 23, 24, 25, 26, −19, 16, −18, 31, 42, −15, −34, −7, −6, −5, −1, 8, −44, 40, 41, −28, −51, 17, 22, −4, −3, 32, 33, 36, −30, −29, 27, −35, −37, 53, 2, −49, 54, −9, 55, 56, −39, −14

Supplementary Fig. 7. The rearrangements analysis in 14 mitochondrial genomes. (A)The rearrangements of the homologous conserved regions. The different color indicated different conserved regions. (B) The matrix of rearrangement blocks.

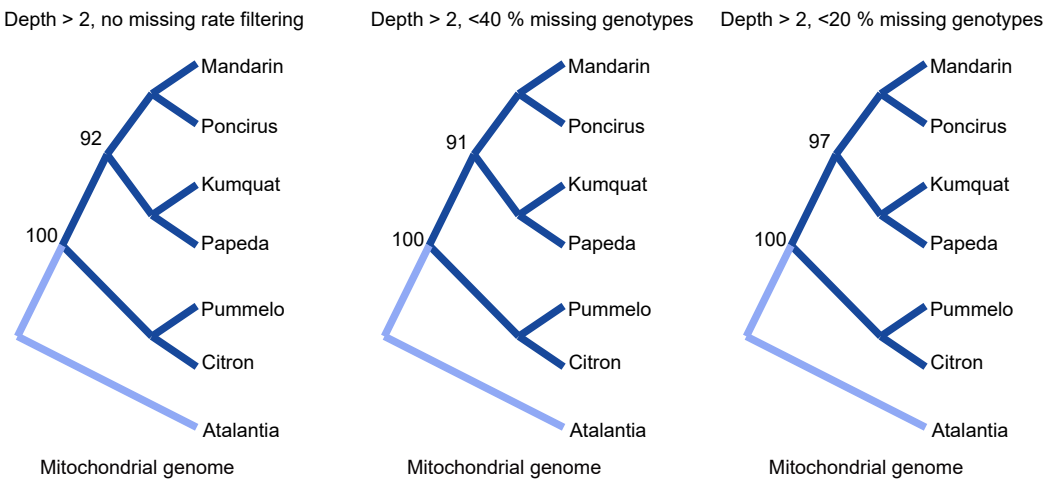

Supplementary Fig. 8. The phylogeny of citrus mitogenome under the nuclear homologous region masking or different missing rate filtering. The corresponding bootstrap value were represented in each phylogenetic tree.

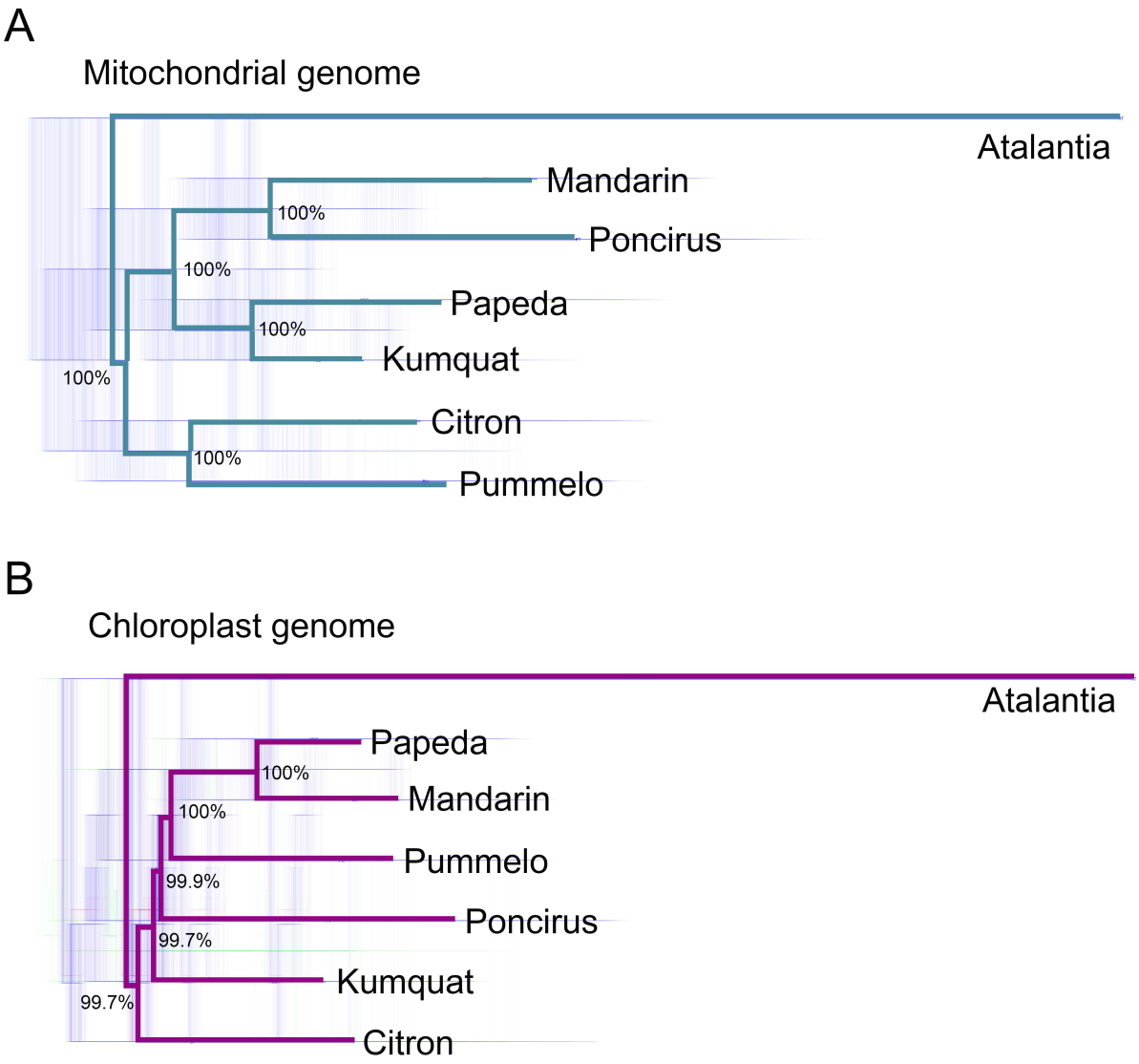

Supplementary Fig. 9. The consensus tree of 1000 individual trees derived from 184 accessions of citrus. (A) The consensus of mitochondrial genome variations, and the probability of each clade was shown. (B) The estimation based on the chloroplast genome variations.

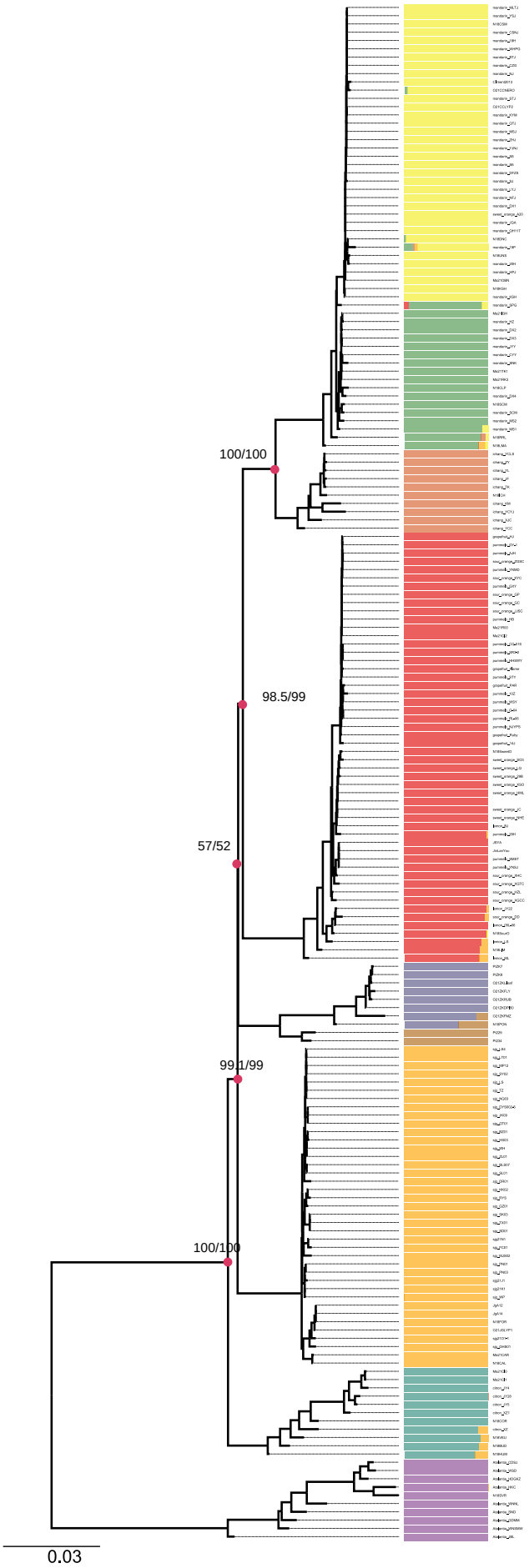

Supplementary Fig. 10. The phylogenetic tree constructed using the chloroplast genomic dataset associated with ancestry component analysis.

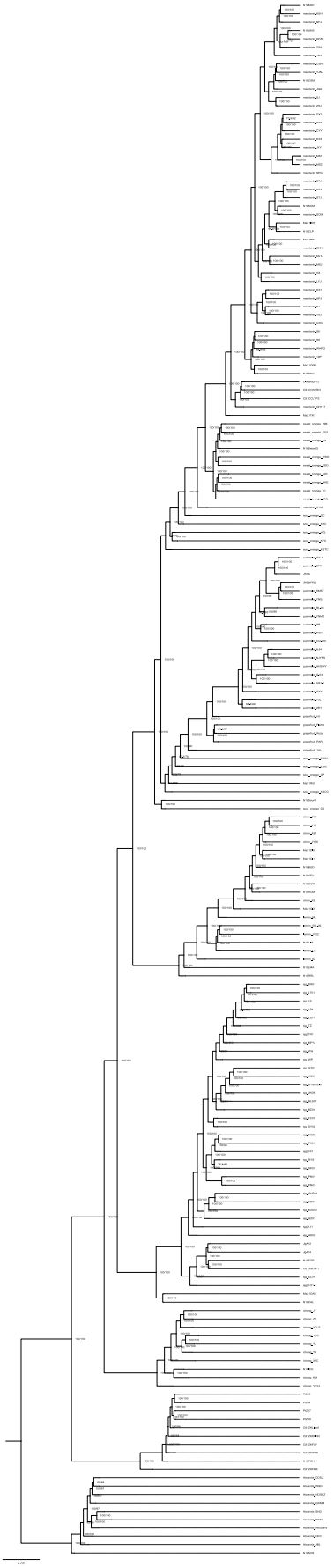

Supplementary Fig. 11. The phylogenetic tree constructed using the nuclear genomic dataset.

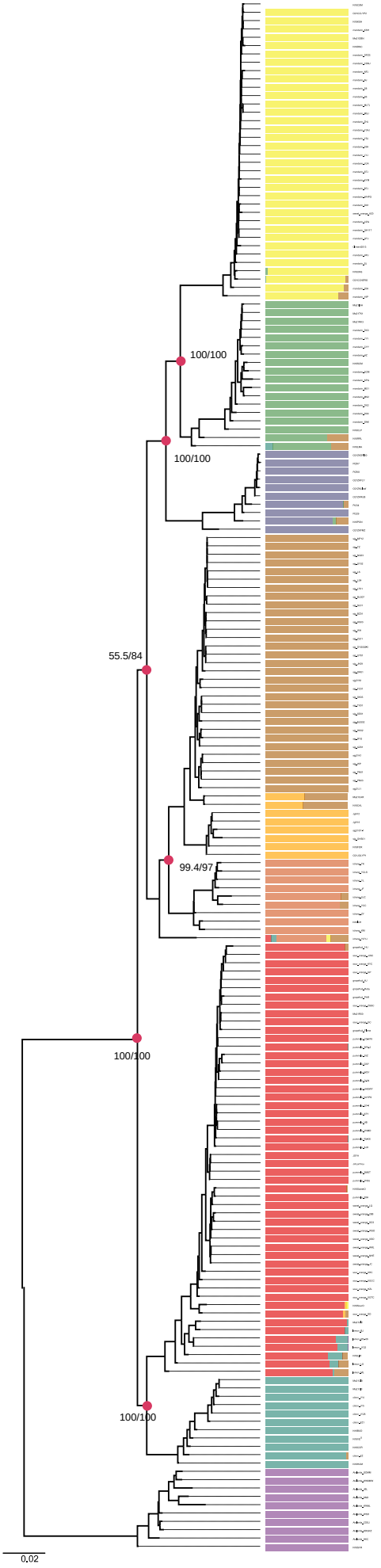

Supplementary Fig. 12. The phylogenetic tree constructed using the mitochondrial genomic dataset associated with ancestry component analysis.

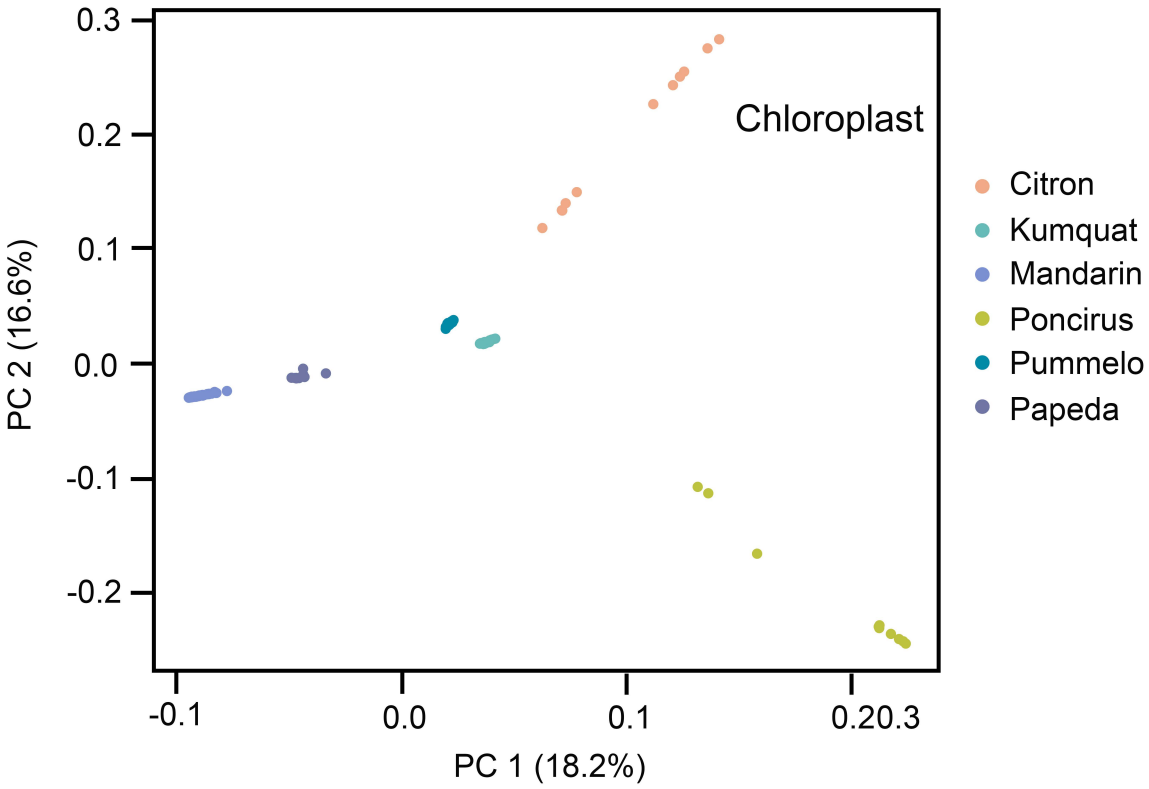

Supplementary Fig. 13. The principal components analysis (PCA) using the chloroplast genomic dataset. The PC1 and PC2 components estimated from chloroplast genomes in six species population were shown. And the hybrid populations were excluded.

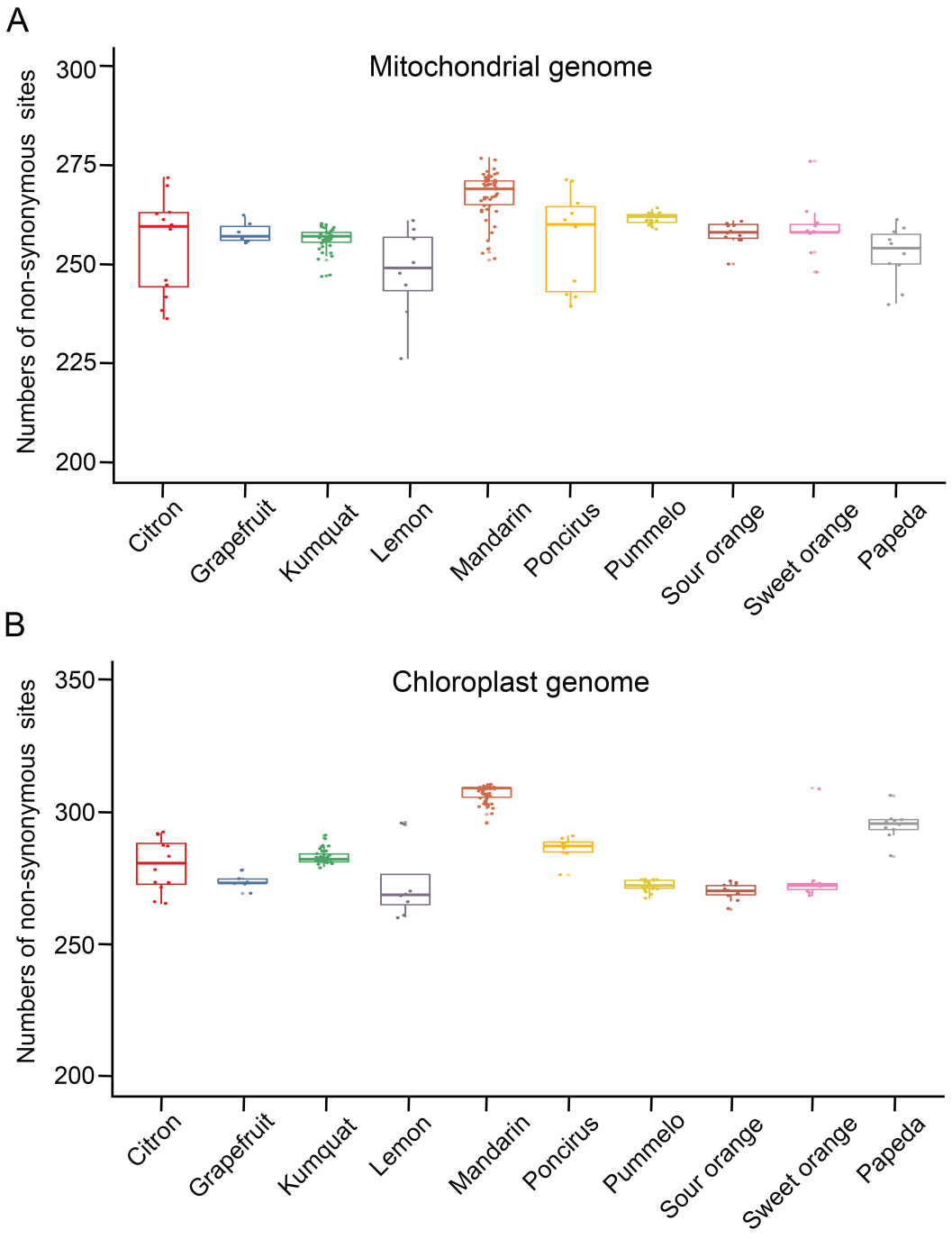

Supplementary Fig. 14. The genetic load estimation in mitochondrial and chloroplast genomes. (A) The number of predicted nonsynonymous sites in the predicted ORFs of the mitochondrial genome in ten populations including hybrid populations. (B) The prediction of genetic load in chloroplast genome. Because the cytoplasmic genomes in the hybrids were inherited from pummelo, the genetic load of hybrids was used as a negative control.

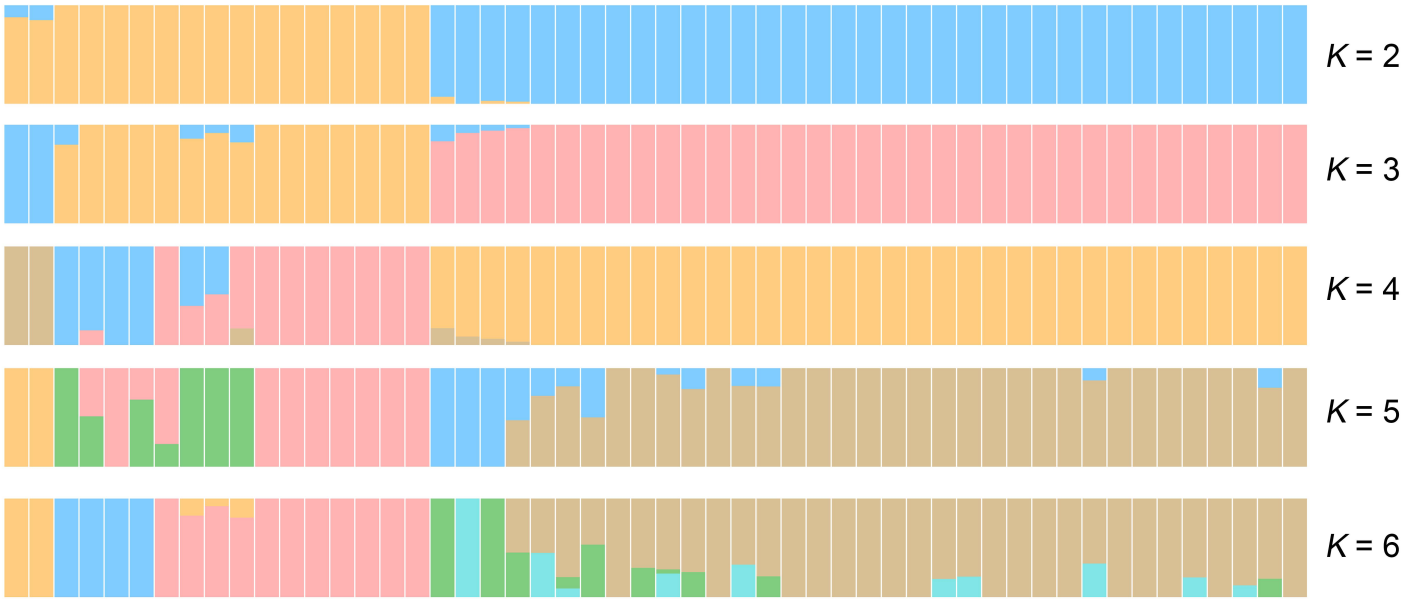

Supplementary Fig. 15. The ancestry composition estimated by mitochondrial genomic dataset in mandarin population. The estimation from *K* = 2 to *K* = 6.

Supplementary Fig. 16. The ancestry composition estimated by nuclear genomic dataset in mandarin population. The estimation from *K* = 2 to *K* = 6.

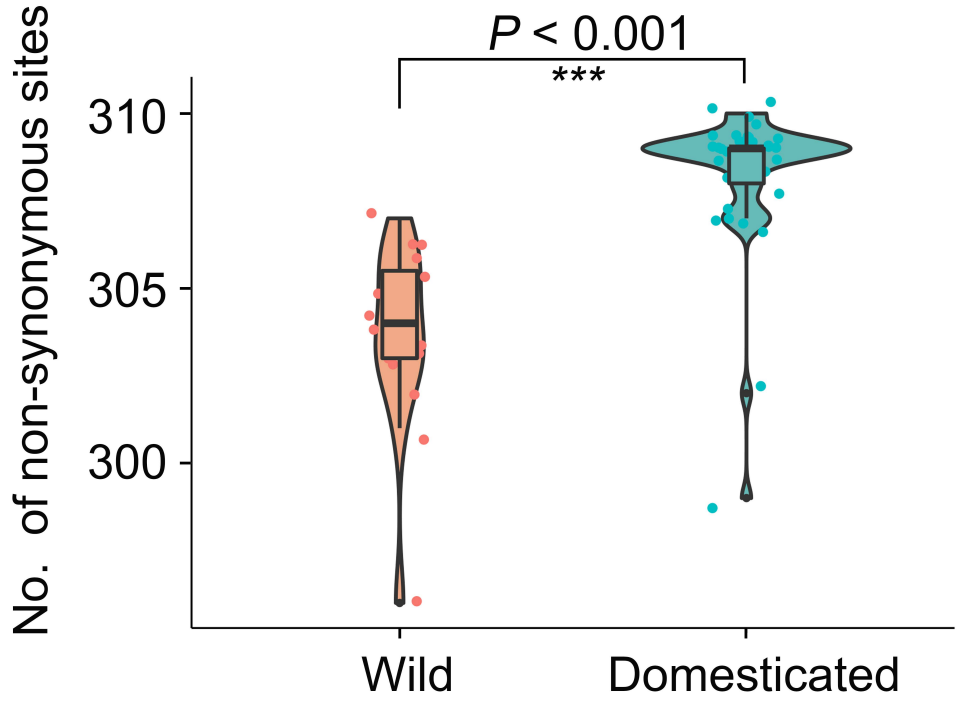

Supplementary Fig. 17. The comparison of genetic load in the chloroplast genome between wild and domesticated mandarins. The wild and domesticated populations was inferred from the chloroplast genomic data. The y-axis indicates the number of non-synonymous sites.

Supplementary Fig. 18. The flowers and anthers at different developmental stages in pummelo cultivar STY and the alloplasmic line G1+STY. The abnormal development that stamens could not reach to the height of stigma could be observed in the G1+STY sample, and the collection of mature anthers showed a dehydrated state.

Supplementary Fig. 19. The flowers between the sweet orange cultivar BTC and the alloplasmic line G1+BTC. There was no difference (stamen height and mature anther status) between the flowers and anthers in the sweet orange cultivar BTC and the alloplasmic line G1+BTC.

A

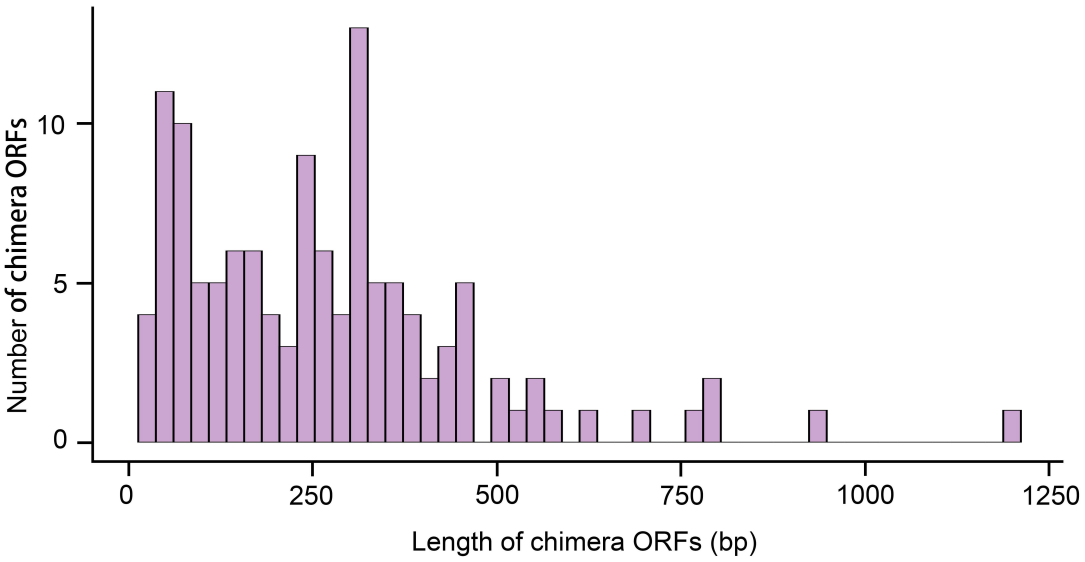

B

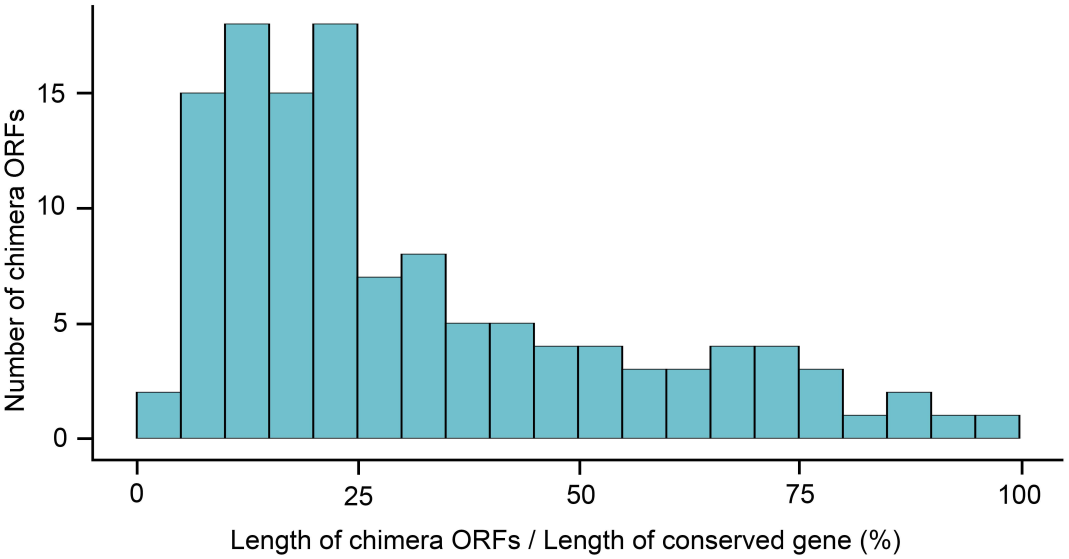

Supplementary Fig. 20. The distribution of chimeric ORFs from conserved genes in mandarin G1 mitochondrial genome. There are two types of chimeric ORFs in the intergenic region, including the shuffling start/stop codons and the splicing fragments. (A) The length distribution of the chimera ORFs. The x-axis indicated the length (bins = 50), while y-axis indicated the number of ORFs. (B) The integrity ratio (length of chimera ORFs/length of related conserved gene) distribution of the chimera ORFs. The x-axis indicated the integrity ratio (%) (bins = 20), while y-axis indicated the number of ORFs.

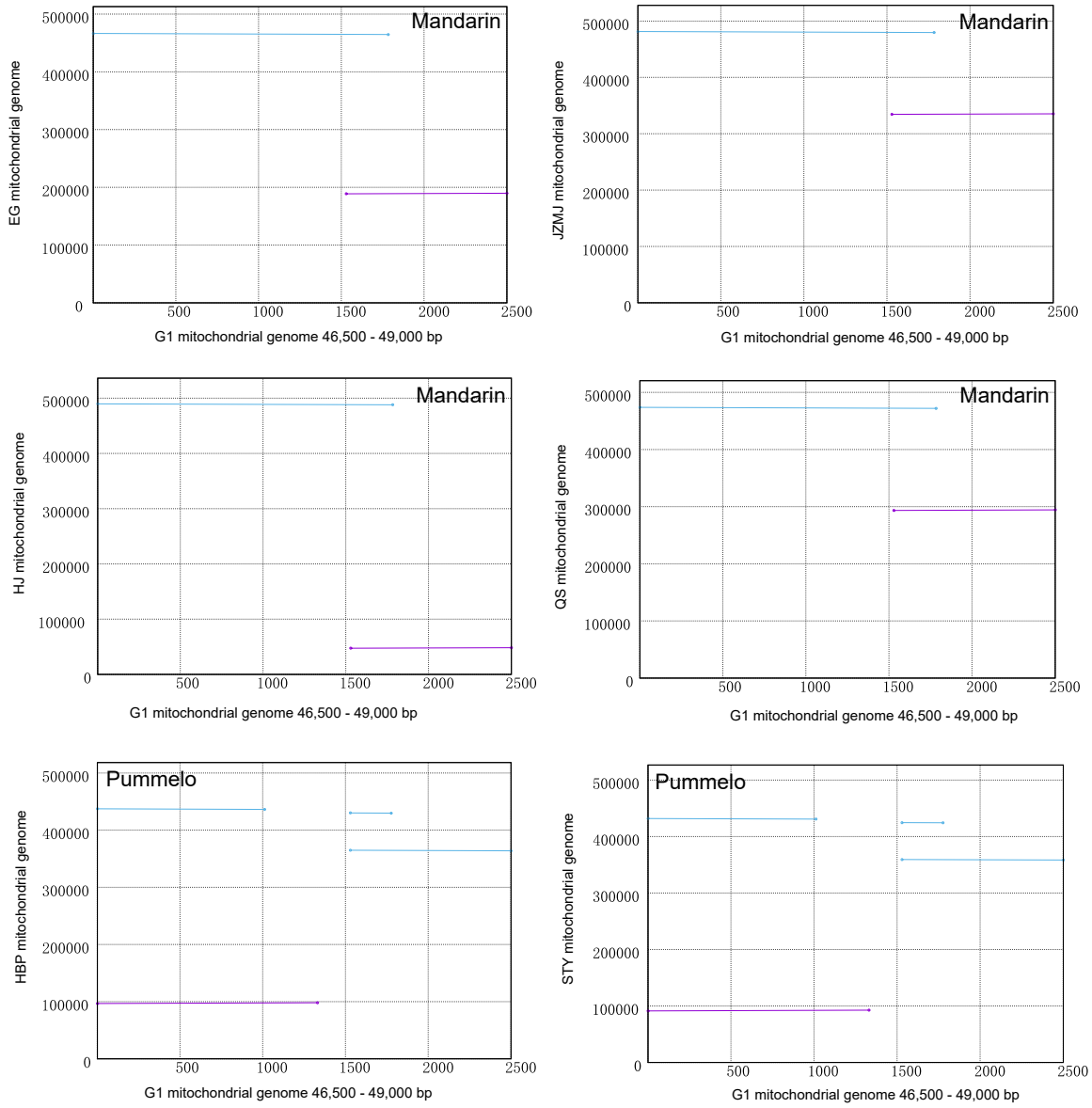

Supplementary Fig. 21. The collinear analysis of orf374 linked region. The *orf374* linked region (46,500 – 49,000 bp) was aligned with the six mitochondrial genomes including four mandarins and two pummelos. The purple indicated the same direction, while blue indicated the opposite arrangements.

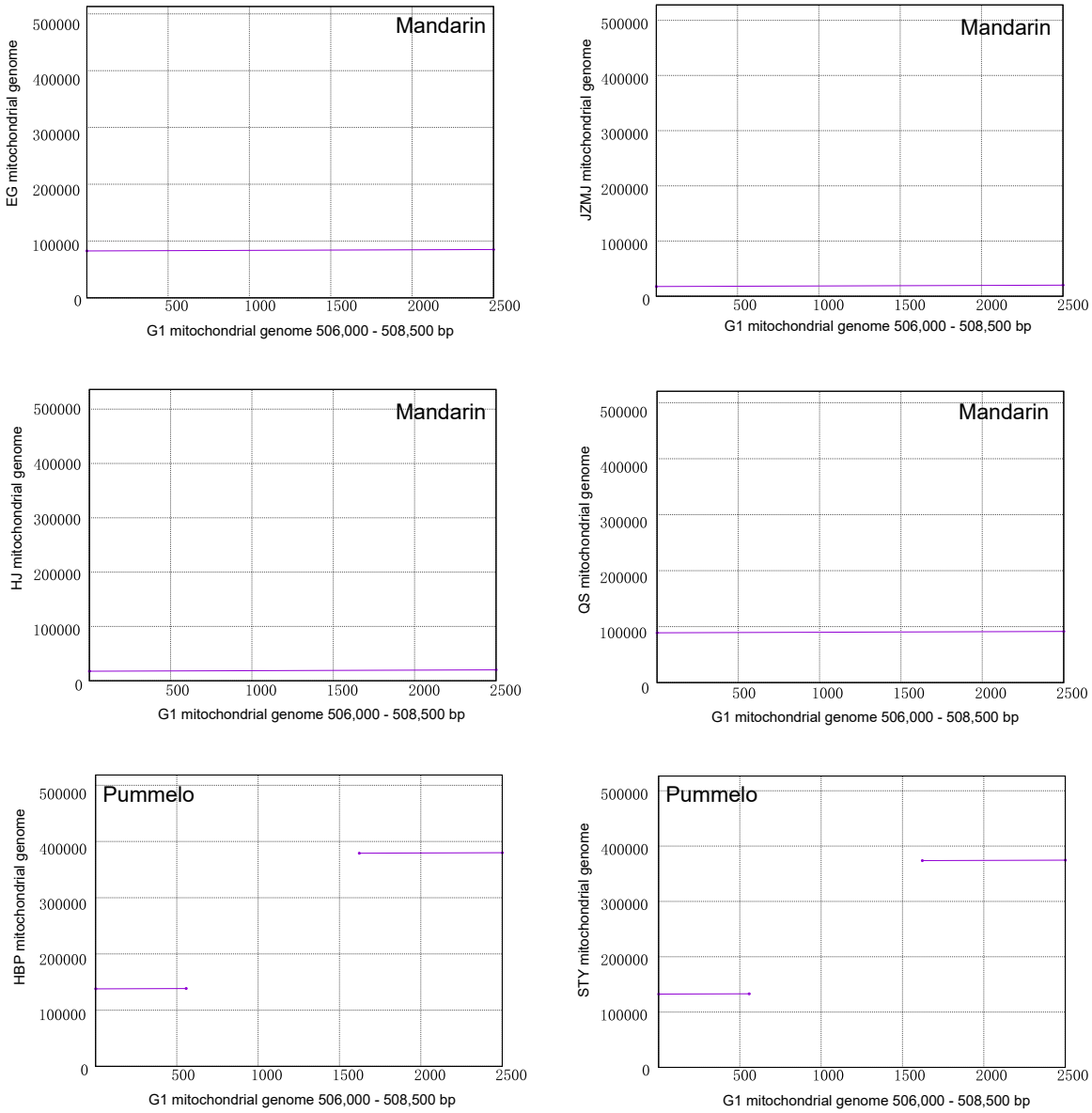

Supplementary Fig. 22. The collinear analysis of orf384 linked region. The *orf384* linked region (506,000 – 508,500 bp) was aligned with the six mitochondrial genomes including four mandarins and two pummelos. The purple indicated the same direction, while blue indicated the opposite arrangements.

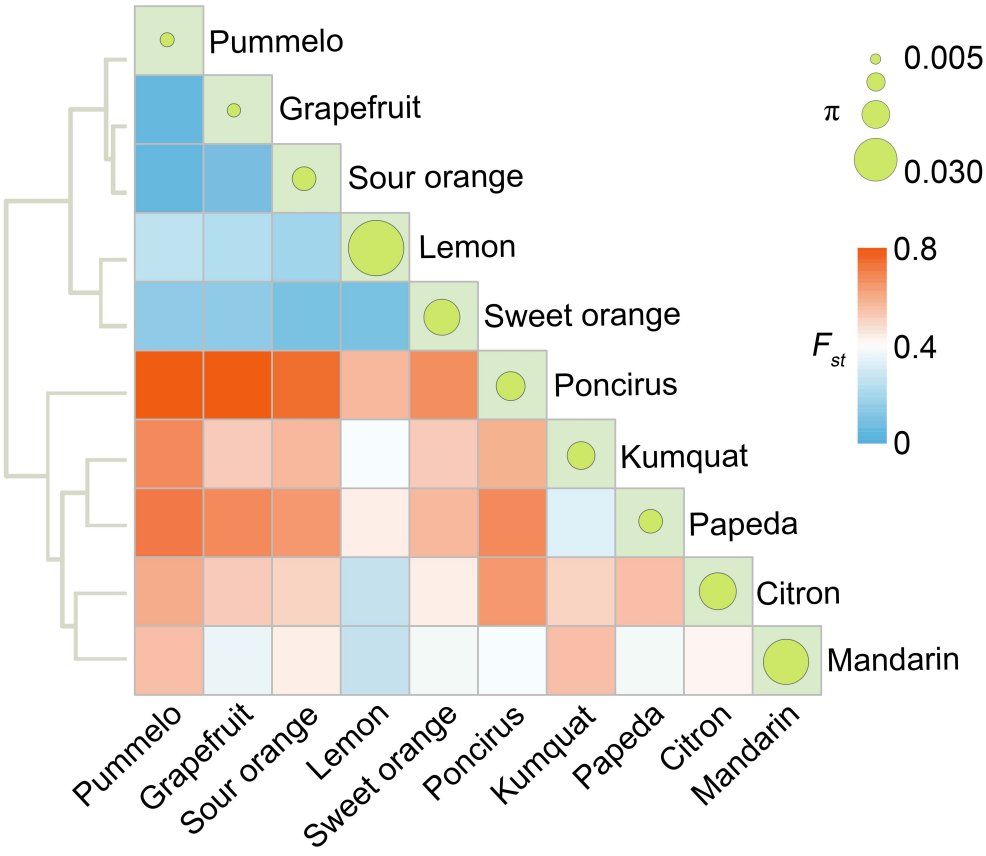

Supplementary Fig. 23. The genetic differentiation in ten populations. The differentiation was estimated by paired F_{st} statistic and ten populations (including the four hybrid populations) were clustered based on F_{st} value. The size of circle presented the genetic diversity (π) value.

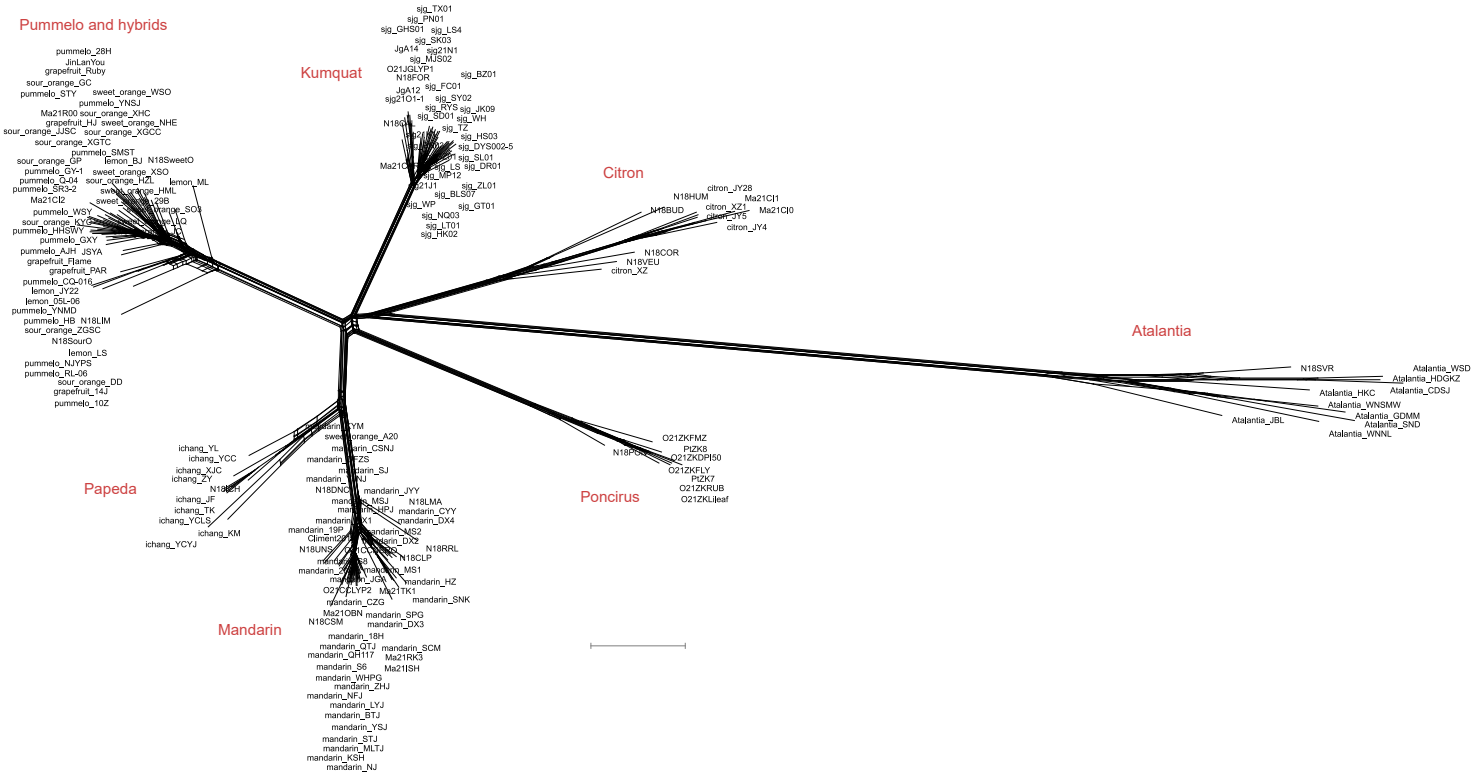

Supplementary Fig. 24. The chloroplast reticulate analysis of 184 accessions in citrus. Four hybrid populations and two hybrid individuals (rangpur lime and rough lemon) were included in the analysis.

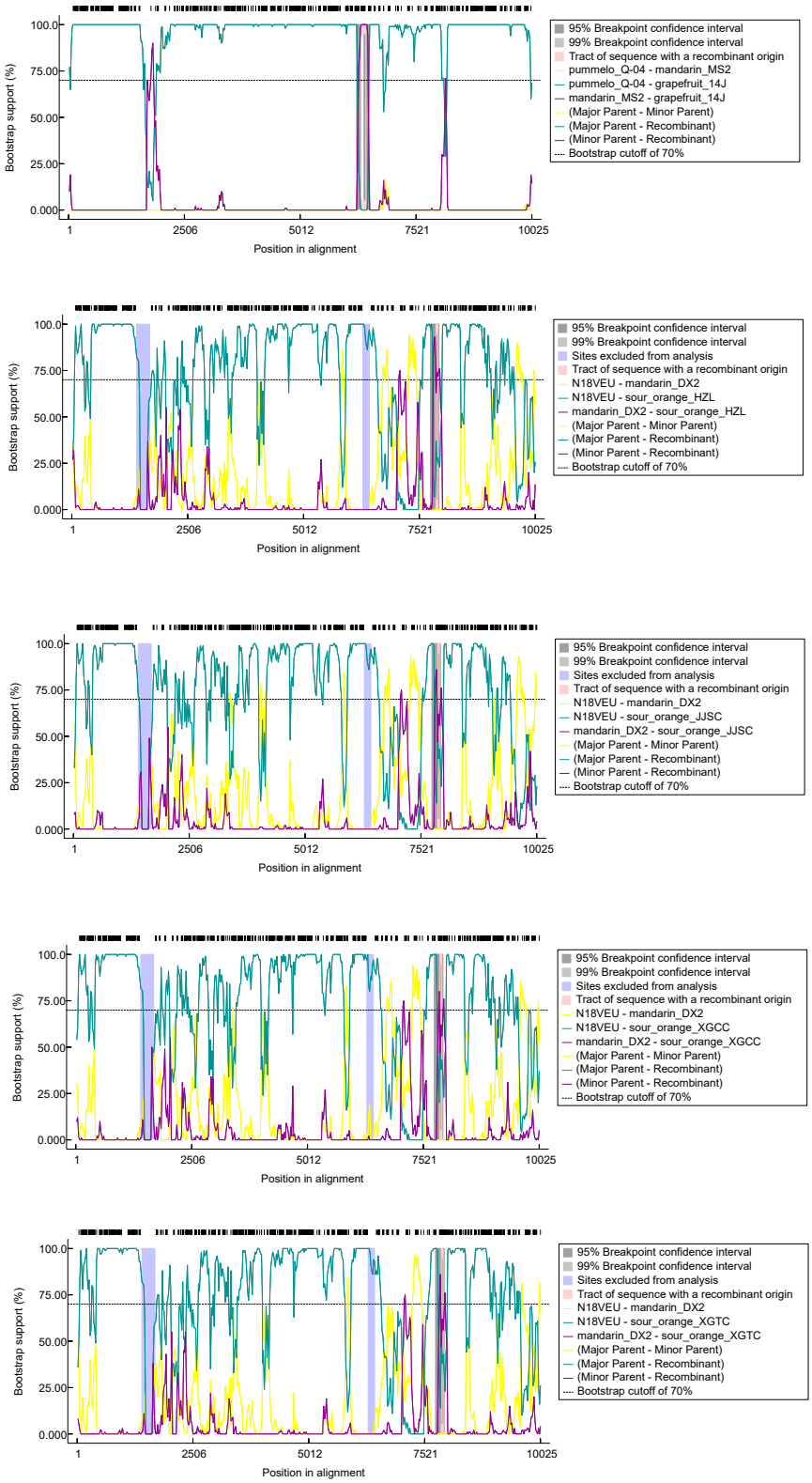

Supplementary Fig. 25. The recombination detected by RDP5. The potential recombination signals (regions) in five samples from grapefruit and sour orange (grapefruit 14J; sour oranges HZL, JJSC, XGCC and XGTC).

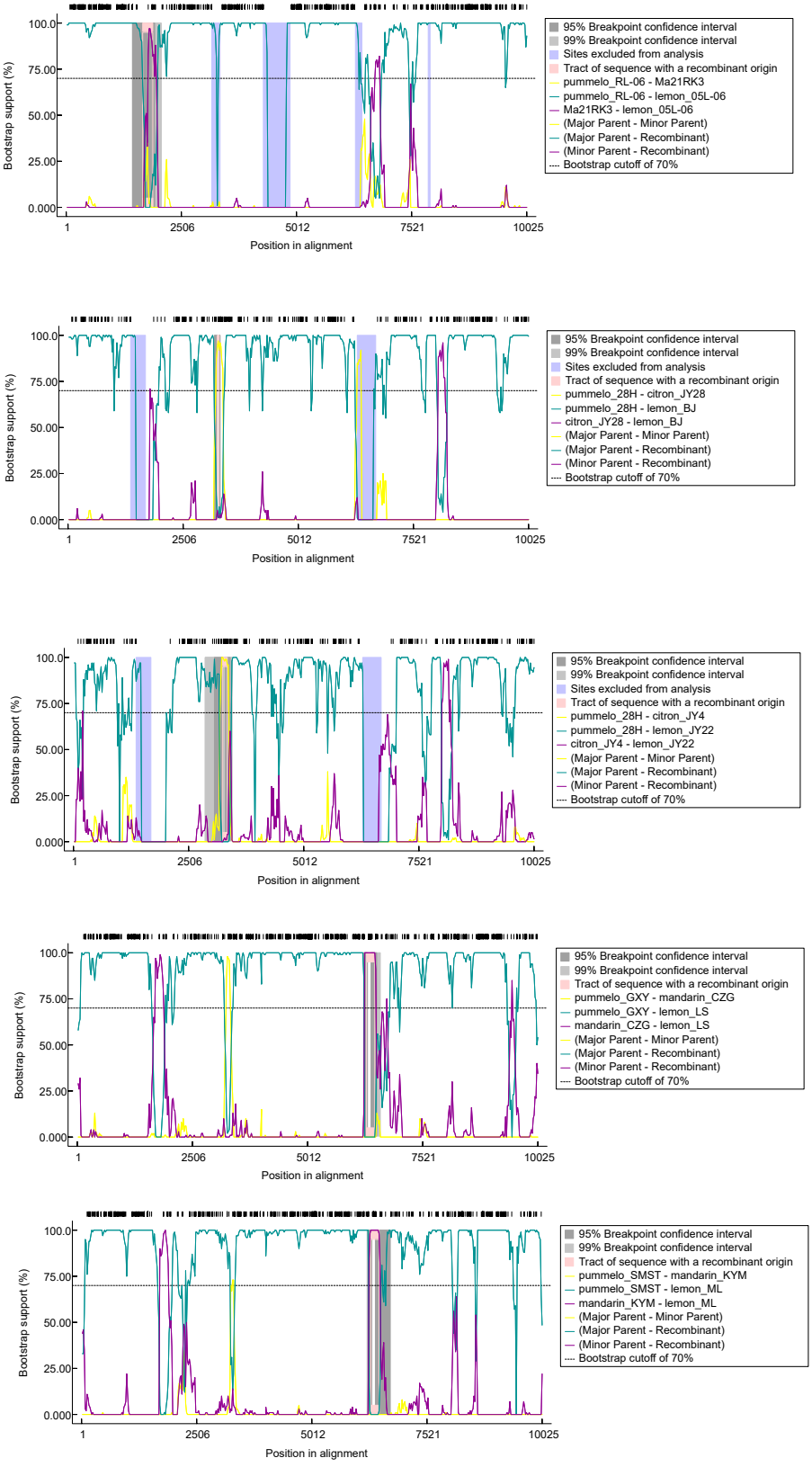

Supplementary Fig. 26. The recombination detected by RDP5. The potential recombination signals (regions) in five lemons (05L-06, BJ, JY22, LS and ML).

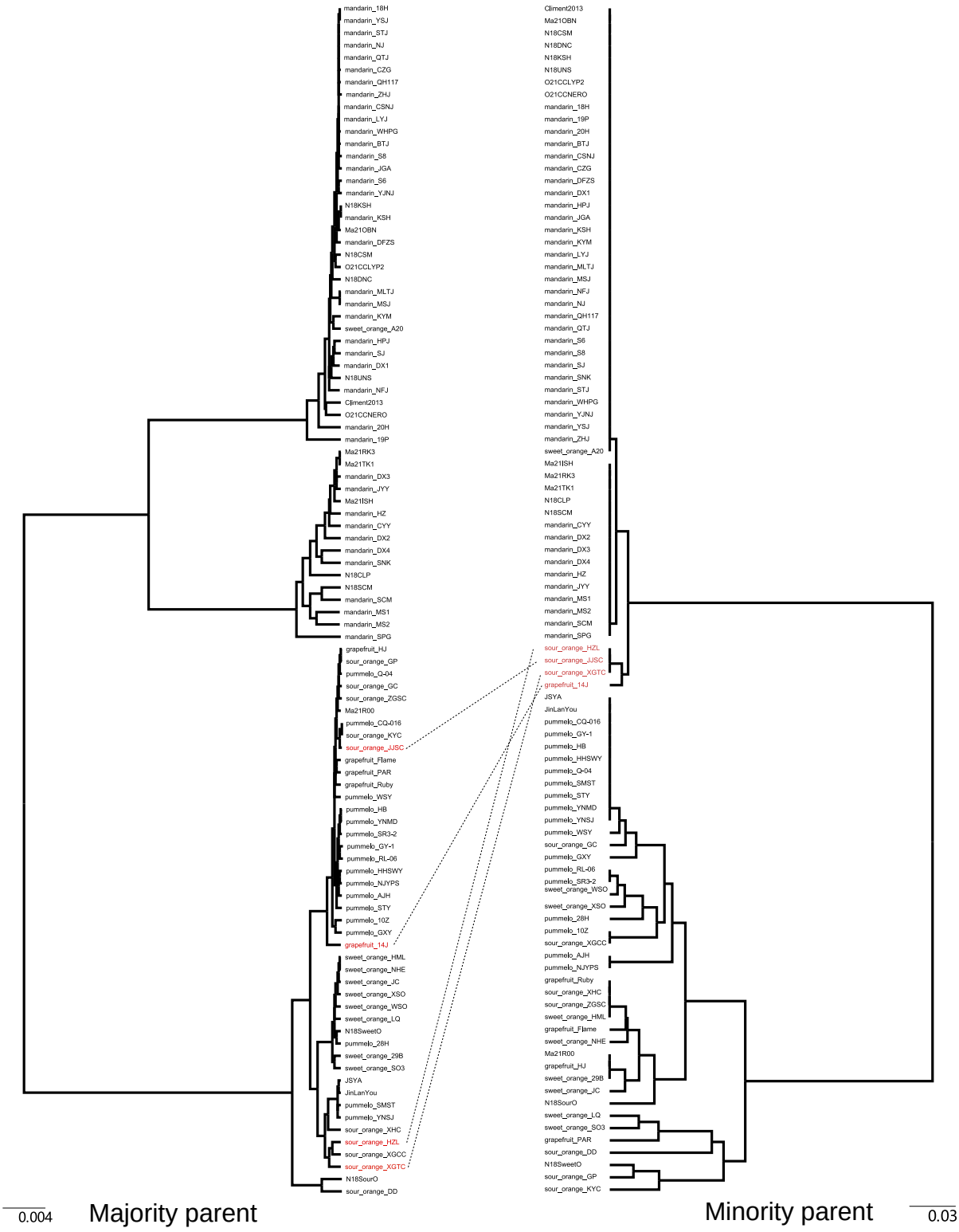

Supplementary Fig. 27. The Maximum Likelihood (ML) phylogeny between the major parent regions and the minor parent regions. The identical topological clade (subgroup1) was connected by dashed line.

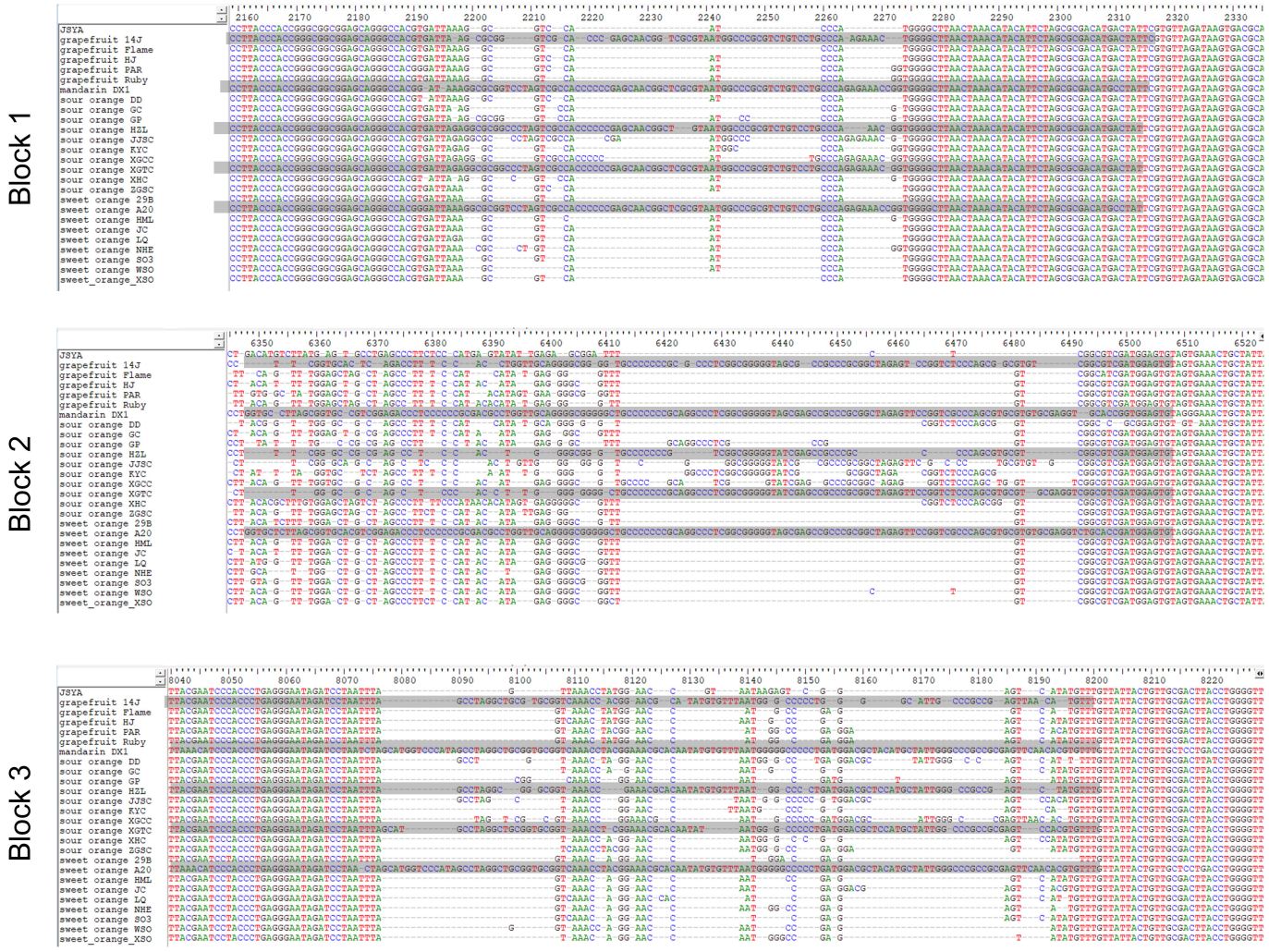

Supplementary Fig. 28. Three recombination blocks associated with deletion/insertion variation. Samples (subgroup1 and subgroup 2) from sour orange and grapefruit populations were plotted and five individuals with heteroplasmy through paternal leakage were highlighted with shadow.

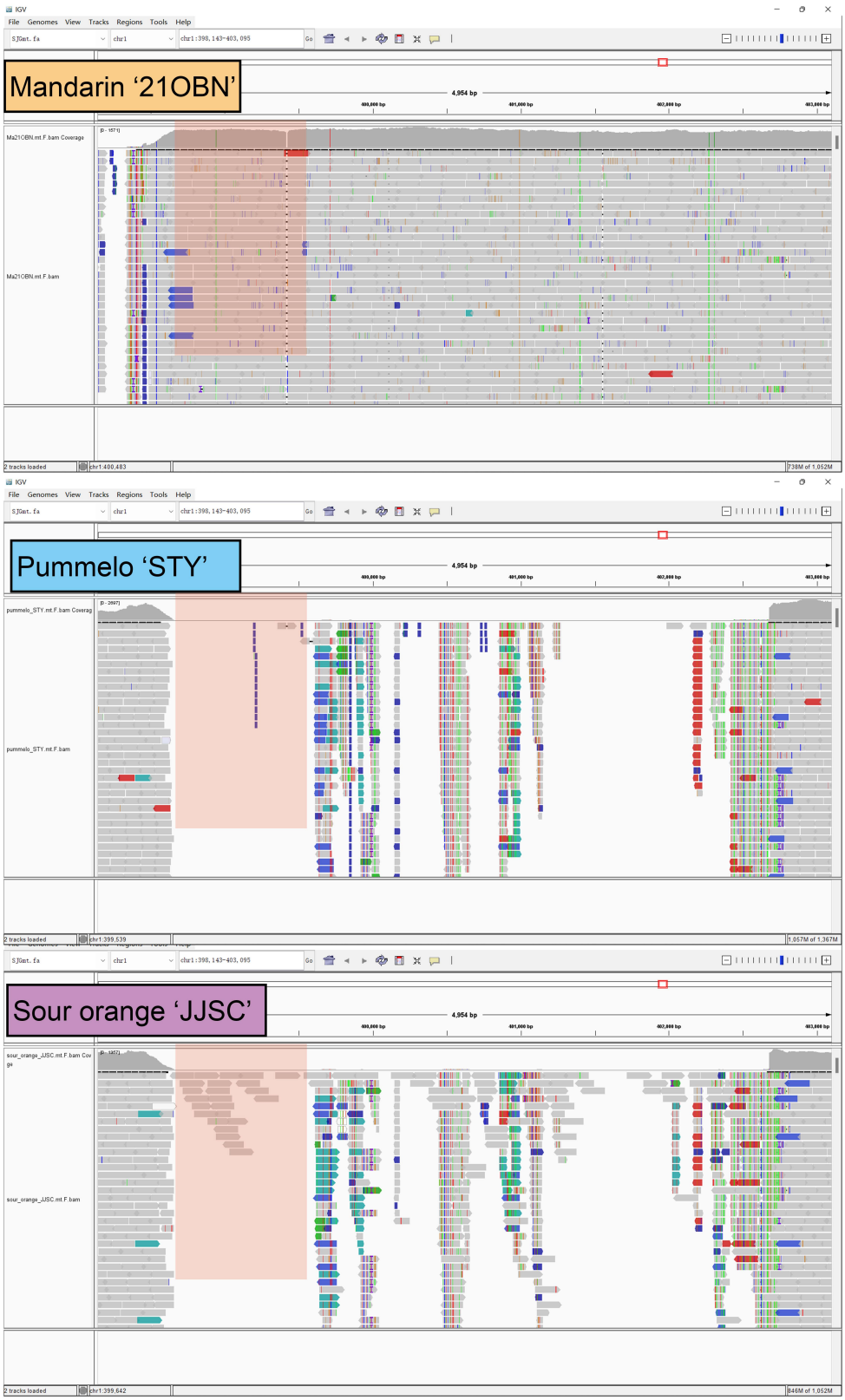

Supplementary Fig. 29. The IGV plot of paternal leakage in sour orange JJSC (subgroup1). The deletion/insertion variation in pummelo and mandarin mitochondrial genomes was identified, with read mapping windows ranging from 398,143 to 403,095 bp. The region with apparent paternal leakage reads was highlighted.

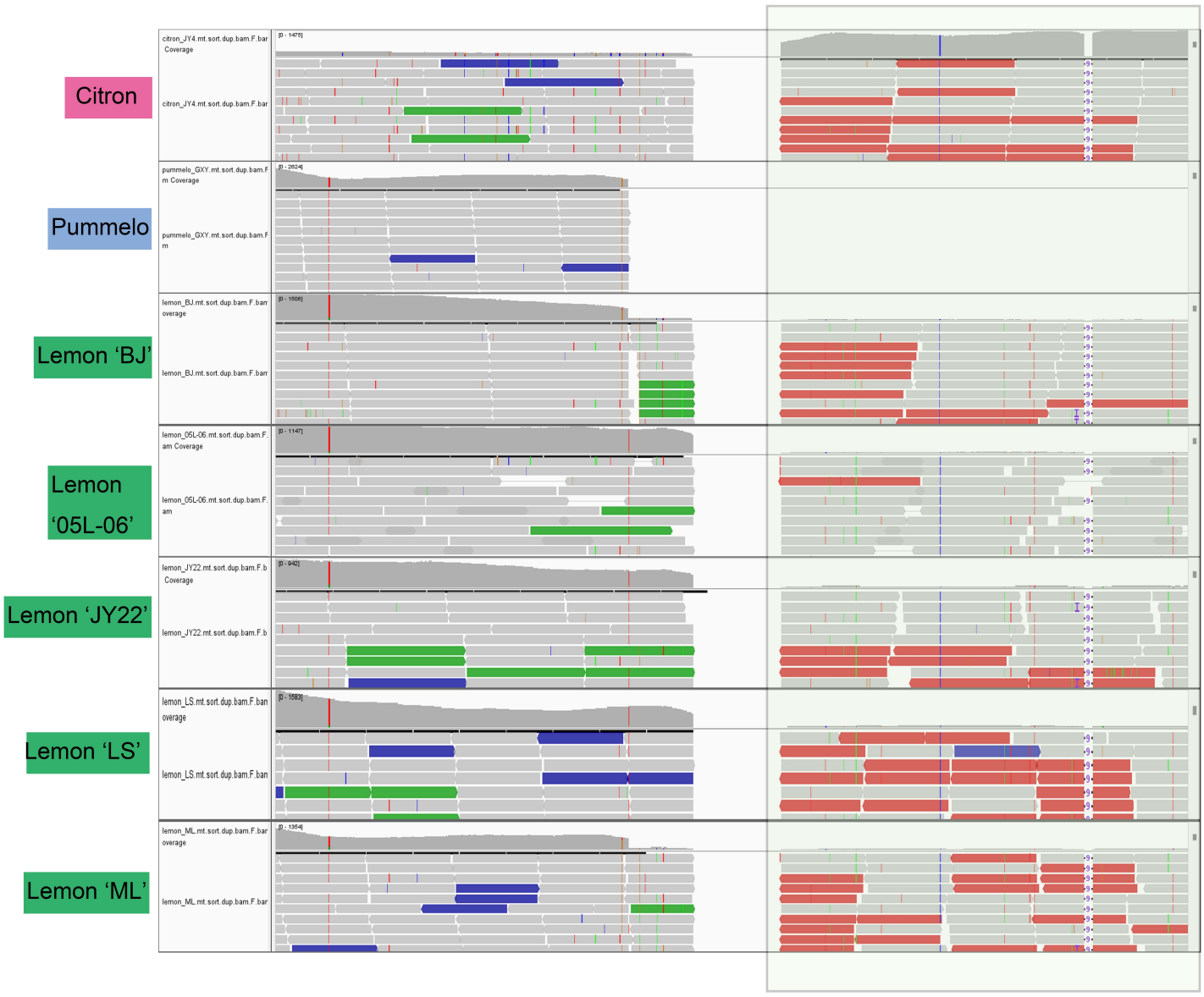

Supplementary Fig. 30. The IGV plot of paternal leakage in lemons. The deletion/insertion variation in pummelo and citron mitochondrial genomes was identified. The region with apparent paternal leakage reads in lemons from the citron was highlighted.

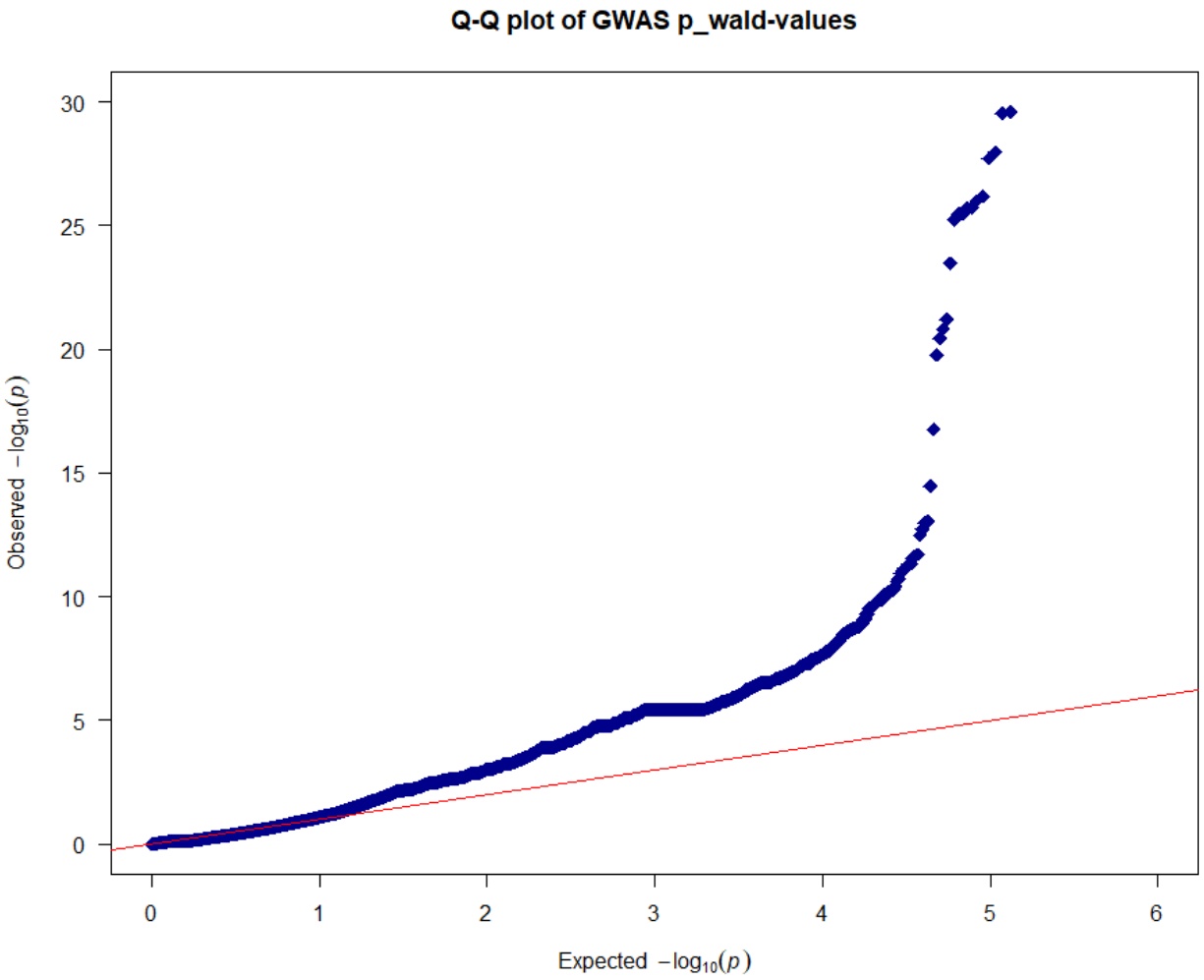

Supplementary Fig. 31. The Q-Q plot of cytoplasmic-nuclear interaction GWAS analysis (*p*_wald value).

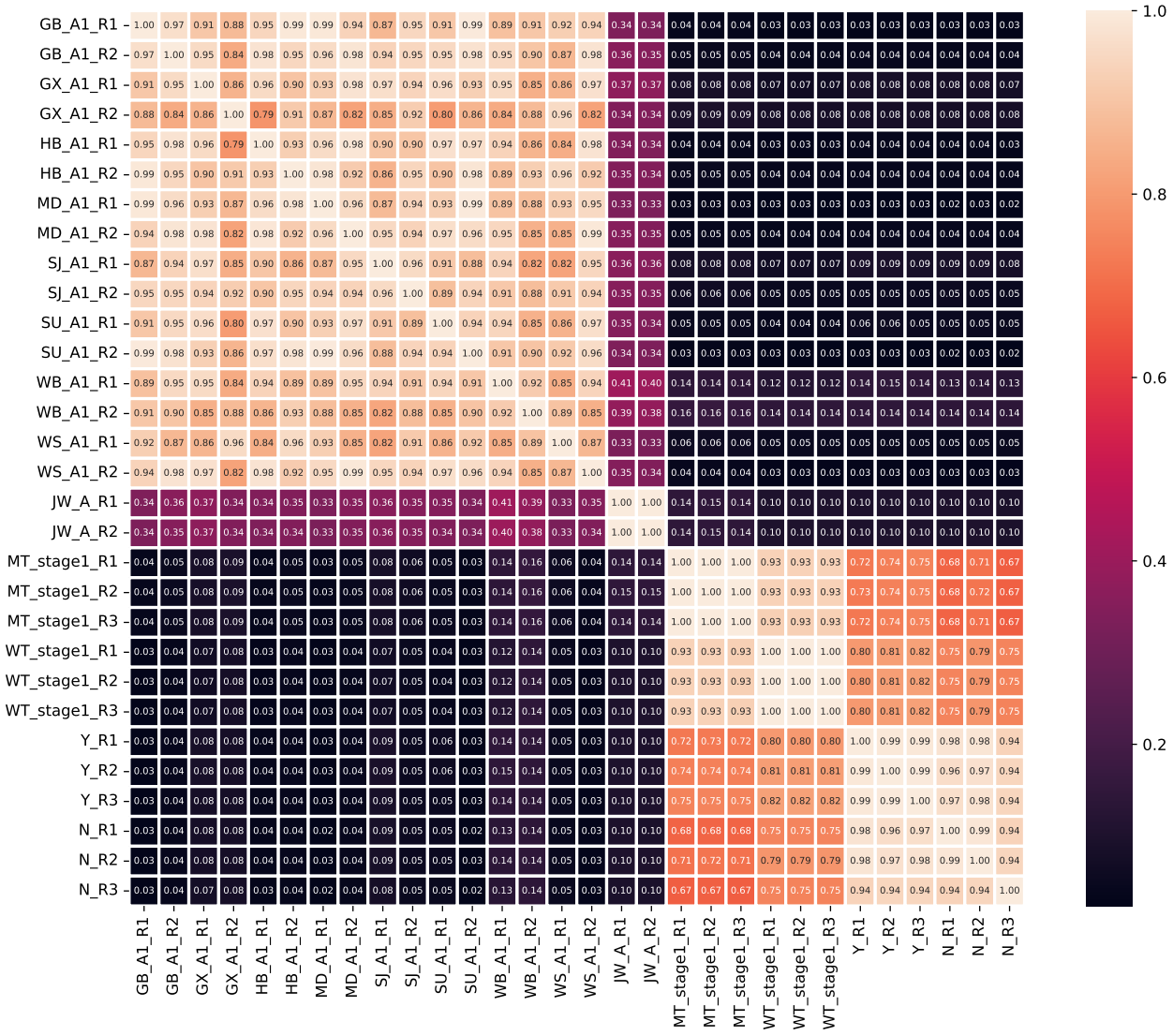

Supplementary Fig. 32. The correlation analysis of anthers from various pummelo and mandarin cultivars. These RNA-seq data were obtained from eight pummelos and four mandarins that published previously. Each pummelo has two biological replicates (_R1 and _R2) and each mandarin has three biological replicates (_R1, _R2 and _R3). The sample JW_A (grapefruit) was used as a negative control. Pummelos: GB, ‘Gaoban’ pummelo; GX, ‘Guanximiyou’ pummelo; HB, HB pummelo; MD, ‘Miandian’ pummelo; SJ, ‘Shuijin’ pummelo; SU, Sour pummelo; WB, ‘Wanbai’ pummelo; WS, Acidless pummelo. Mandarins: WT_stage1, Ponkan mandarin; MT_stage1, Seedless Ponkan mandarin; Y, Ougan; N, ‘Wuzi’ ougan (the SRR list see Supplementary table 9).

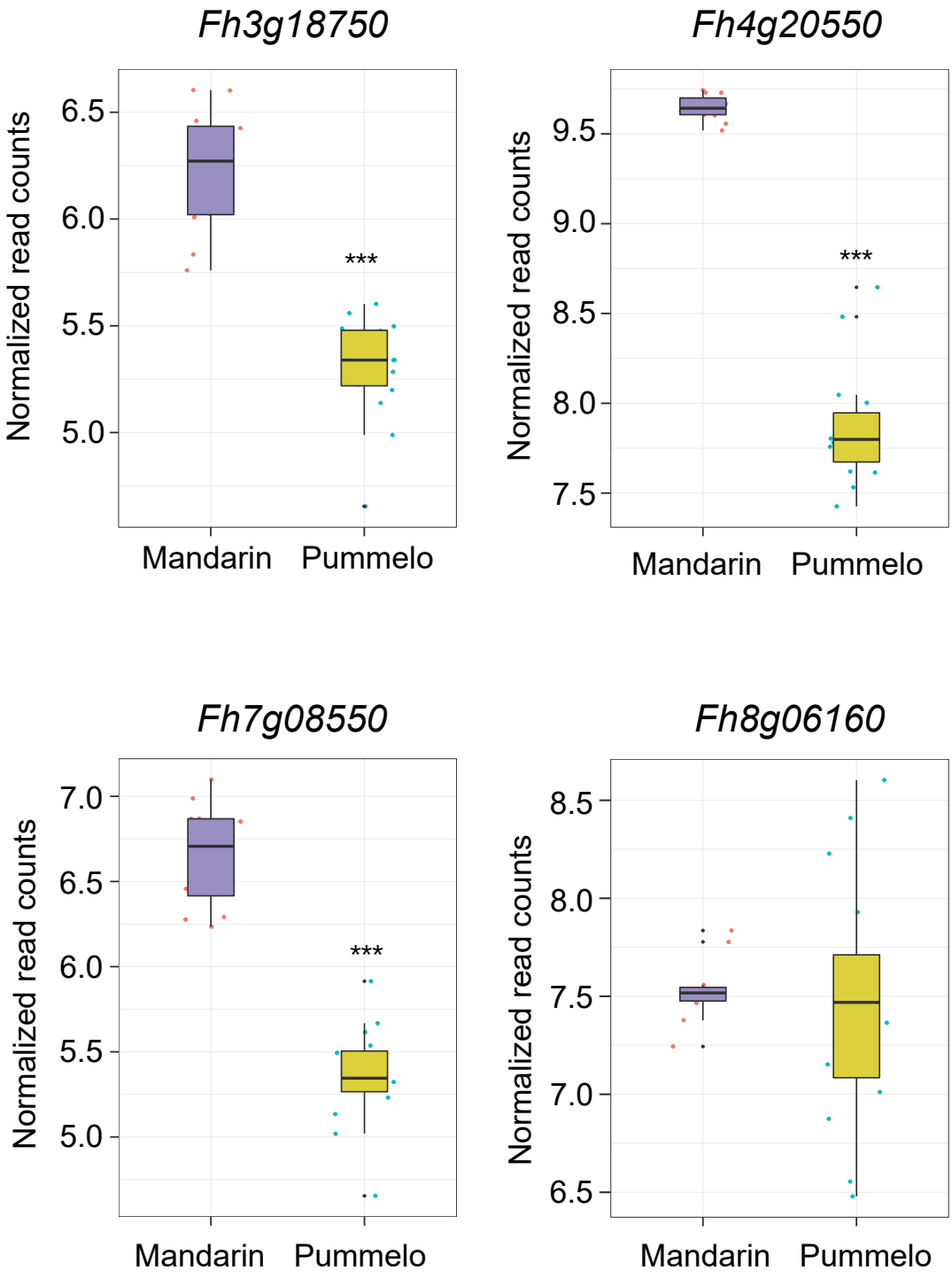

Supplementary Fig. 33. Expression of four PPR genes in anthers under cytoplasmic-nuclear interaction GWAS analysis. The expression levels of three PPR genes were significantly higher expressed in mandarin than in pummelo (FDR adjusted ****p* <0.001). The y-axis represents normalized read counts based on the genome-wide expression matrix.

Supplementary Table 1. The statistics of data used for mitochondrial genome assembling and reads mapping.

Number	Accession ID	Species name	Catalog	Catalog	Platform	Number of reads	Total bases (Gb)	Average length of reads (bp)	Maximum length of reads (bp)	Cite	Source
1	BDGJ	*Citrus reticulata* (Blanco)	mandarin	Bendiguang	nanopore	362310	7.58	20932.6	114564	this study	PRJNA807745
1	BDGJ	*Citrus reticulata* (Blanco)	mandarin	Bendiguang	illumina	34680236	5.20	150	150	this study	PRJNA807745
2	BTC	*Citrus sinensis* (Osbeck)	sweet orange	Bingtang	pacbio	1184308	34.62	29235.3	779454	Wang et al. 2021	PRJNA321100
2	BTC	*Citrus sinensis* (Osbeck)	sweet orange	Bingtang	illumina	97396780	14.41	148	150	Wang et al. 2021	PRJNA321100
3	EG	*Citrus reticulata*	mandarin	Egan	pacbio	351168	6.93	19745.8	243893	this study	PRJNA807745
3	EG	*Citrus reticulata*	mandarin	Egan	illumina	9792964	1.47	150	150	this study	PRJNA807745
4	G1	*Citrus unshiu* Macf.	mandarin	Guoqing No.1	pacbio	496241	5.26	10598.7	83563	Zhang et al. 2020	PRJNA598773
4	HBP	*Citrus grandis*	pummelo	Hirado Butan	pacbio	601567	6.45	10723.7	90852	Zhang et al. 2020	PRJNA598773
5	HJ	*Citrus reticulata* (Blanco)	mandarin	Hongju	nanopore	411901	6.40	15543.5	96172	this study	PRJNA807745
5	HJ	*Citrus reticulata* (Blanco)	mandarin	Hongju	illumina	30687038	4.60	150	150	this study	PRJNA807745
6	HKC	*Atalantia buxifolia*	atalantia	Haokeci	pacbio	7611333	25.59	3361.4	164214	Wang et al. 2017	PRJNA327148
6	HKC	*Atalantia buxifolia*	atalantia	Haokeci	illumina	103877216	10.38	99.9	100	Wang et al. 2017	PRJNA327148
7	JW	*Citrus paradisi Macf.*	grapefruit	Cocktail	illumina	11283382	1.69	150	150	this study	PRJNA807745
8	JZMJ	*Citrus reticulata* (Blanco)	mandarin	Jizhoumi	nanopore	634000	9.71	15313.6	115344	this study	PRJNA807745
8	JZMJ	*Citrus reticulata* (Blanco)	mandarin	Jizhoumi	illumina	55906288	8.39	150	150	this study	PRJNA807745
9	QS	*Citrus reticulata*	mandarin	Qianyang	pacbio	451098	8.19	18153.4	251650	this study	PRJNA807745
9	QS	*Citrus reticulata*	mandarin	Qianyang	illumina	9832964	1.47	150	150	this study	PRJNA807745
10	SJG	*Fortunella hindsii*	kumquat	Shanjingan	pacbio	551765	12.00	21748.4	112888	Zhu et al. 2019	PRJNA487160
10	SJG	*Fortunella hindsii*	kumquat	Shanjingan	illumina	76420022	10.76	149	150	Zhu et al. 2019	PRJNA487160
11	STY	*Citrus grandis*	pummelo	Shatian	nanopore	644776	11.85	18371.6	154762	this study	PRJNA807745
11	STY	*Citrus grandis*	pummelo	Shatian	illumina	53832782	8.07	150	150	this study	PRJNA807745
12	YLK	*Citrus limon* (L.) Burm.f.	lemon	Eureka	nanopore	1808657	27.90	15427.9	536885	this study	PRJNA807745
12	YLK	*Citrus limon* (L.) Burm.f.	lemon	Eureka	illumina	6654594	1.00	150	150	this study	PRJNA807745
13	ZK	*Poncirus trifoliata*	poncirus	Zhike	pacbio	3372157	30.49	9040.3	143717	Huang et al. 2021	VKKW00000000
13	ZK	*Poncirus trifoliata*	poncirus	Zhike	illumina	10629494	1.59	150	150	this study	PRJNA807745

References:
1. Wang X, et al. (2017) Genomic analyses of primitive, wild and cultivated citrus provide insights into asexual reproduction. *Nature Genetics* 49(5):765-772.
2. Zhu C, et al. (2019) Genome sequencing and CRISPR/Cas9 gene editing of an early flowering Mini-Citrus (*Fortunella hindsii*). *Plant Biotechnology Journal* 17(11): 2199-2210.
3. Zhang S, et al. (2020) Assembly of Satsuma mandarin mitochondrial genome and identification of cytoplasmic male sterility–specific ORFs in a somatic cybrid of pummelo. *Tree Genetics & Genomes* 16(6):1-13.
4. Wang L, et al. (2021) Somatic variations led to the selection of acidic and acidless orange cultivars. *Nature Plants* 7(7):954-965.
5. Huang Y, et al. (2021) Genome of a citrus rootstock and global DNA demethylation caused by heterografting. *Horticulure Research* 8(1):69.

Supplementary Table 2. The statistics of 16 assemblies and mitochondrial Pan-genome.

Accessions	Size (bp)	GC (%)	Repeat sequences	Gaps	Number of conserved protein genes	Length of coding region (bp)	Number of tRNAs	Length of tRNAs (bp)	Number of rRNAs
HKC	449354	44.72	5446 bp (1.21 %)	13	34	30667	24	1801	3
YLK	509002	45.05	5158 bp (1.01 %)	9	35	30383	26	1935	3
EG	512938	45.13	5567 bp (1.09 %)	1	37	30582	26	1934	3
BTC	513691	45.04	5226 bp (0.99 %)	9	36	30705	25	1870	3
BDGJ	519536	45.12	5303 bp (1.02 %)	1	36	30646	26	1935	3
JW	519898	44.99	5244 bp (1.01 %)	11	36	32437	27	2015	3
SJG	520158	45.05	5919 bp (1.14 %)	0	35	29470	26	1918	3
QS	520466	45.04	5742 bp (1.10 %)	3	37	32248	26	1937	3
STY	526596	45.08	5054 bp (0.98 %)	2	36	30568	26	1935	3
JZMJ	527901	44.95	5640 bp (1.07 %)	2	37	31076	26	1934	3
ZK	533342	44.95	5683 bp (1.07 %)	0	35	30829	25	1866	3
HJ	536281	44.68	5543 bp (1.03 %)	2	36	32309	31	2330	3
HBP*	518274	45.14	5218 bp (1.01 %)	0	36	29921	26	1935	3
G1*	521559	45.06	5592 bp (1.07 %)	0	37	30361	26	1934	3
Pan-genome	670817	44.12	7638 bp (1.14 %)	——	——	——	——	——	——

References:
1. Zhang S, et al. (2020) Assembly of Satsuma mandarin mitochondrial genome and identification of cytoplasmic male sterility–specific ORFs in a somatic cybrid of pummelo. *Tree Genetics & Genomes* 16(6):1-13.

Supplementary Table 3. The primers used for filling gaps in kumquat SJG and poncirus ZK assemblies.

Name of primer	Forward primer	Reverse primer	Assemble
filling-gaps-16F	AGCCCGTGCGAATGAAAG	TCAGCGAGGAAATGGGAACA	SJG
filling-gaps-518F	TGCGGTGCTAACGATTTA	GCTCATACCTCCTTCCCGAAAC	SJG
filling-gaps-1158F	AGGCACTGGTCACGGGTAGG	CGGCGTCAAGCATTCGTT	SJG
filling-gaps-3F	GCGTAGTGGGAATAGCCCC	TCCCGCAATAACTCGGCATCT	ZK
filling-gaps-1F	TGCCGTTTCATCCTTTCGT	TTATCCGAAGGGCACGCA	ZK

Supplementary Table 4. The homologous region between conserved genes (trans-splicing fragments) and chimera prodicted ORFs in the intergenic region of mandarin G1 mitogenome.

Accession	Classification	Number	Type	Homologous	Length (bp)	Start (bp)	End (bp)
HKC	Atalantia	1	pridicted ORF on HKC mitogenome	f45	381	118875	119255
			conserved gene	nad3	354	67516	67163
		2	pridicted ORF on HKC mitogenome	f56	1230	122787	124016
			conserved gene	atp8	477	443506	443982
		3	pridicted ORF on HKC mitogenome	r488	894	27771	28664
			conserved gene	rps4	1044	153760	154803
ZK	Poncirus	1	pridicted ORF on ZK mitogenome	f286	336	209447	209782
			trans-splicing fragment	nad5_fragment_1	237	291625	291389
		2	pridicted ORF on ZK mitogenome	f1197	921	97501	98421
			conserved gene	rps4	1044	457118	458161
		3	pridicted ORF on ZK mitogenome	r1080	357	502116	502472
			conserved gene	nad3	354	223260	222907
		4	pridicted ORF on ZK mitogenome	f781	1017	405577	406593
			trans-splicing fragment	nad5_fragment_1	237	291625	291389
		5	pridicted ORF on ZK mitogenome	f1152	711	7897	8607
			conserved gene	sdh3	291	211650	211360
		6	pridicted ORF on ZK mitogenome	r182	654	166380	167033
			trans-splicing fragment	ccmFc_fragment_1	771	190432	189662
JG	Kumquat	1	pridicted ORF on JG mitogenome	r1228	276	86903	87178
			trans-splicing fragment	ccmFc_fragment_1	771	482922	483692
		2	pridicted ORF on JG mitogenome	r74	339	119365	119703
			conserved gene	rps4	1044	118898	119941
		3	pridicted ORF on JG mitogenome	f474	834	273581	274414
			conserved gene	atp8	477	86124	85648
		4	pridicted ORF on JG mitogenome	r832	975	407870	408844
			conserved gene	rps4	1044	118898	119941
		5	pridicted ORF on JG mitogenome	r1105	1956	44162	46117
			conserved gene	atp1	1521	464498	466018

EG	Mandarin	1	pridicted ORF on EG mitogenome	r23	783	108612	109394
			conserved gene	atp8	477	82232	81756
		2	pridicted ORF on EG mitogenome	r510	984	291608	292591
			conserved gene	rps4	1044	320020	321063
		3	pridicted ORF on EG mitogenome	f988	1104	464670	465773
			trans-splicing fragment	nad5_fragment_1	237	188906	188670
		4	pridicted ORF on EG mitogenome	r1168 (*orf384*)	1155	83068	84222
			trans-splicing fragment	nad5_fragment_1	237	188906	188670
JZMJ	Mandarin	1	pridicted ORF on JZMJ mitogenome	r379	783	254262	255044
			conserved gene	atp8	477	17287	16811
		2	pridicted ORF on JZMJ mitogenome	f1007	1104	479633	480736
			trans-splicing fragment	nad5_fragment_1	237	334547	334311
		3	pridicted ORF on JZMJ mitogenome	r1200	306	95298	95603
			conserved gene	matR	1983	96499	94517
		4	pridicted ORF on JZMJ mitogenome	r88	984	134722	135705
			conserved gene	rps4	1044	163134	164177
		5	pridicted ORF on JZMJ mitogenome	r204 (*orf384*)	1155	18123	19277
			trans-splicing fragment	nad5_fragment_1	237	334547	334311
HJ	Mandarin	1	pridicted ORF on HJ mitogenome	f1021	1104	488013	489116
			trans-splicing fragment	nad5_fragment_1	237	47485	47249
		2	pridicted ORF on HJ mitogenome	r419	783	269727	270509
			conserved gene	atp8	477	17287	16811
		3	pridicted ORF on HJ mitogenome	r205(*orf384*)	1155	18123	19277
			trans-splicing fragment	nad5_fragment_1	237	47485	47249
		4	pridicted ORF on HJ mitogenome	r130	984	150187	151170
			conserved gene	rps4	1044	178599	179642
QS	Mandarin	1	pridicted ORF on QS mitogenome	f364	1080	242920	243999
			conserved gene	sdh3	291	243208	243498
		2	pridicted ORF on QS mitogenome	f976	1104	471971	473074
			trans-splicing fragment	nad5_fragment_1	237	293443	293207
		3	pridicted ORF on QS mitogenome	r1229(*orf384*)	1155	89452	90606
			trans-splicing fragment	nad5_fragment_1	237	293443	293207

		4	pridicted ORF on QS mitogenome	r280	783	213162	213944
			conserved gene	atp8	477	88616	88140
		5	pridicted ORF on QS mitogenome	f591	984	324289	325272
			conserved gene	rps4	1044	122034	123077
G1	Mandarin	1	pridicted ORF on G1 mitogenome	r427	783	270337	271119
			conserved gene	atp8	477	505681	505205
		2	pridicted ORF on G1 mitogenome	r127	984	150797	151780
			conserved gene	rps4	1044	179209	180252
		3	pridicted ORF on G1 mitogenome	r982(*orf374*)	1122	47166	48287
			trans-splicing fragment	nad5_fragment_1	237	350616	350380
		4	pridicted ORF on G1 mitogenome	r1084(*orf384*)	1155	506517	507671
			trans-splicing fragment	nad5_fragment_1	237	350616	350380
HBP	Pummelo	1	pridicted ORF on HBP mitogenome	r810	381	400209	400589
			conserved gene	nad3	354	95406	95053
		2	pridicted ORF on HBP mitogenome	f876	1104	429840	430943
			trans-splicing fragment	nad5_fragment_1	237	364762	364998
		3	pridicted ORF on HBP mitogenome	r969	975	46452	47426
			conserved gene	rps4	1044	447416	448459
		4	pridicted ORF on HBP mitogenome	r1222	1965	95539	97503
			conserved gene	atp1	1521	436754	438274
		5	pridicted ORF on HBP mitogenome	r800	450	397870	398319
			conserved gene	atp8	477	137569	137093
		6	pridicted ORF on HBP mitogenome	f75	507	138388	138894
			trans-splicing fragment	ccmFc_fragment_1	771	28793	28023
STY	Pummelo	1	pridicted ORF on STY mitogenome	r805	381	394740	395120
			conserved gene	nad3	354	89715	89362
		2	pridicted ORF on STY mitogenome	r1226	1629	90411	92039
			conserved gene	atp1	1521	431285	432805
		3	pridicted ORF on STY mitogenome	f62	507	132930	133436
			trans-splicing fragment	ccmFc_fragment_1	771	23109	22339
		4	pridicted ORF on STY mitogenome	f872	1104	424371	425474
			trans-splicing fragment	nad5_fragment_1	237	359292	359528

		5	pridicted ORF on STY mitogenome	r833	975	40768	41742
			conserved gene	rps4	1044	441947	442990
		6	pridicted ORF on STY mitogenome	r794	450	392401	392850
			conserved gene	atp8	477	132111	131635
YLK	Hybrid	1	pridicted ORF on YLK mitogenome	f931	975	461550	462524
			conserved gene	rps4	1044	384286	385329
		2	pridicted ORF on YLK mitogenome	f699	921	366893	367813
			trans-splicing fragment	nad5_fragment_1	237	265884	266120
		3	pridicted ORF on YLK mitogenome	r912	1965	45490	47454
			conserved gene	atp1	1521	373624	375144
		4	pridicted ORF on YLK mitogenome	r201	1653	180530	182182
			trans-splicing fragment	nad5_fragment_1	237	265884	266120
		5	pridicted ORF on YLK mitogenome	f271	381	211445	211825
			conserved gene	nad3	354	45357	45004
		6	pridicted ORF on YLK mitogenome	r1194	903	91314	92216
			trans-splicing fragment	ccmFc_fragment_1	771	480188	480958
		7	pridicted ORF on YLK mitogenome	f281	450	213715	214164
			conserved gene	atp8	477	90752	90276
BTC	Hybrid	1	pridicted ORF on BTC mitogenome	f716	1104	379171	380274
			trans-splicing fragment	nad5_fragment_1	237	314092	314328
		2	pridicted ORF on BTC mitogenome	r649	381	349540	349920
			conserved gene	nad3	354	41003	40650
		3	pridicted ORF on BTC mitogenome	r959	813	466526	467338
			conserved gene	rps4	1044	61973	62903
		4	pridicted ORF on BTC mitogenome	f112	507	151850	152356
			trans-splicing fragment	ccmFc_fragment_1	771	484899	485669
		5	pridicted ORF on BTC mitogenome	r639	450	347201	347650
			conserved gene	atp8	477	151031	150555
		1	pridicted ORF on JW mitogenome	r811	450	416231	416680
			conserved gene	atp8	477	89491	89015
		2	pridicted ORF on JW mitogenome	f1207	507	90310	90816
			trans-splicing fragment	ccmFc_fragment_1	771	491105	491875

JW	Hybrid	3	pridicted ORF on JW mitogenome	r955	813	472732	473544
			conserved gene	rps4	930	158755	159685
		4	pridicted ORF on JW mitogenome	f584	339	316837	317175
			conserved gene	matR	1983	316871	314889
		5	pridicted ORF on JW mitogenome	r821	381	418570	418950
			conserved gene	nad3	354	48631	48278
		6	pridicted ORF on JW mitogenome	f918	1104	448201	449304
			trans-splicing fragment	nad5_fragment_1	237	383122	383358
BDGJ	Hybrid	1	pridicted ORF on BDGJ mitogenome	r275	1104	196970	198073
			trans-splicing fragment	nad5_fragment_1	237	263152	262916
		2	pridicted ORF on BDGJ mitogenome	r249	1965	189336	191300
			conserved gene	atp1	1521	461557	463077
		3	pridicted ORF on BDGJ mitogenome	r866	507	420023	420529
			trans-splicing fragment	ccmFc_fragment_1	771	490744	491514
		4	pridicted ORF on BDGJ mitogenome	f987	975	472111	473085
			conserved gene	rps4	1044	281443	280400
		5	pridicted ORF on BDGJ mitogenome	f339	450	229594	230043
			conserved gene	atp8	477	421348	421824
		6	pridicted ORF on BDGJ mitogenome	f328	381	227324	227704
			conserved gene	nad3	354	189203	188850

Notes:

1. The chimera ORFs were homologus but not overlapped with conserved genes or trans-splicing fragments (in the intergenic region). The position (start and end) was based on each mitogenome.
2. The predicted ORF *orf374* was displayed with purple, while the predicted ORF *orf384* was displayed with green.
3. The SRRs of previous non coding RNA-seq data from HBP, G1 and the alloplasmic G1+HBP were SRR10828043, SRR10821405 and SRR10841903, respectively.
4. The SRRs of newly sequencing non coding RNA-seq from BTC and the alloplasmic G1+BTC were SRR20645581 and SRR20645582, respectively.

Supplementary Table 5. The identified SVs by assemblies' alignment and long reads mapping.

Position (bp)	Types	Information	Genotypes												
			HKC	JW	YLK	BDGJ	EG	G1	HJ	JZMJ	QS	ZK	HBP	STY	BTC
53331	<DEL>	SVTYPE=DEL;END=54188;LEN=857	1	0	0	0	0	0	0	0	0	0	0	0	0
53349	<INV>	SVTYPE=INV;END=95521;LEN=42172	0	0	0	0	0	1	0	0	0	0	0	0	0
53360	<INS>	SVTYPE=INS;END=53486;LEN=101	0	1	0	0	0	0	0	0	0	0	0	1	0
53486	<DEL>	SVTYPE=DEL;END=54786;LEN=1300	0	0	0	0	0	0	0	0	0	0	0	0	1
54786	<DUP>	SVTYPE=DUP;END=54912;LEN=126	0	1	0	0	0	0	0	0	0	0	0	0	0
74571	<DEL>	SVTYPE=DEL;END=76435;LEN=1864	0	1	0	0	0	0	0	0	0	0	0	0	0
82284	<INV>	SVTYPE=INV;END=115598;LEN=33314	1	0	0	0	0	0	0	0	0	0	0	0	0
87485	<INS>	SVTYPE=INS;END=87735;LEN=3474	0	0	1	0	0	0	0	0	0	0	0	0	0
95521	<INV>	SVTYPE=INV;END=119658;LEN=24137	0	0	0	0	0	0	0	0	1	0	0	0	0
104293	<INV>	SVTYPE=INV;END=127531;LEN=23238	0	1	0	0	0	0	0	0	0	0	0	0	0
104293	<INV>	SVTYPE=INV;END=178427;LEN=74134	0	0	1	0	0	0	0	0	0	0	0	0	0
104293	<INV>	SVTYPE=INV;END=119658;LEN=15365	0	0	0	0	1	0	1	1	0	0	0	0	0
104293	<INS>	SVTYPE=INS;END=178922;LEN=544	0	0	0	0	0	0	0	0	0	0	1	1	0
118239	<INS>	SVTYPE=INS;END=118252;LEN=15788	0	0	0	0	0	1	0	0	0	0	0	0	0
118252	<INS>	SVTYPE=INS;END=126989;LEN=815	1	0	0	0	0	0	0	0	0	0	0	0	0
119658	<INV>	SVTYPE=INV;END=157606;LEN=37949	0	0	0	0	0	1	0	0	0	0	0	0	0
173142	<INV>	SVTYPE=INV;END=228845;LEN=55703	1	0	0	0	0	0	0	0	0	0	0	0	0
173602	<INV>	SVTYPE=INV;END=225254;LEN=51652	0	0	0	0	0	0	0	0	1	0	0	0	0
173602	<INV>	SVTYPE=INV;END=352163;LEN=178561	0	0	0	0	0	0	1	1	0	0	0	0	0
173650	<INV>	SVTYPE=INV;END=228845;LEN=55195	0	0	0	1	0	0	0	0	0	0	0	0	0
173650	<INV>	SVTYPE=INV;END=293166;LEN=119516	0	1	0	0	0	0	0	0	0	0	0	0	0
204624	<INV>	SVTYPE=INV;END=396033;LEN=191409	0	0	0	0	1	0	0	0	0	0	0	0	0
204624	<INV>	SVTYPE=INV;END=293166;LEN=88542	0	0	0	0	0	0	0	0	0	0	1	1	0
225462	<INV>	SVTYPE=INV;END=281615;LEN=56153	0	0	1	0	0	0	0	0	0	0	0	0	0
225462	<INV>	SVTYPE=INV;END=293166;LEN=67704	0	0	0	0	0	0	0	0	0	0	0	0	1
228845	<INV>	SVTYPE=INV;END=282179;LEN=53334	0	0	0	0	0	0	0	0	0	1	0	0	0
228845	<INV>	SVTYPE=INV;END=280184;LEN=51339	0	0	0	0	0	0	0	0	0	0	1	1	0
265424	<INV>	SVTYPE=INV;END=300925;LEN=35501	0	0	0	0	0	0	0	0	1	0	0	0	0
265424	<INS>	SVTYPE=INS;END=300925;LEN=20081	0	0	0	0	0	1	0	0	0	0	0	0	0
280957	<INV>	SVTYPE=INV;END=337799;LEN=56842	1	0	0	0	0	0	0	0	0	0	0	0	0
293442	<INV>	SVTYPE=INV;END=351911;LEN=58469	0	0	0	1	0	0	0	0	0	0	0	0	0
317808	<INV>	SVTYPE=INV;END=380156;LEN=62348	0	0	0	0	0	0	0	0	1	0	0	0	0
317815	<INS>	SVTYPE=INS;END=382423;LEN=106	0	0	0	0	0	0	0	0	1	0	0	0	0
338046	<DEL>	SVTYPE=DEL;END=472283;LEN=134237	0	0	0	0	0	1	0	0	0	0	0	0	0

345824	<INV>	SVTYPE=INV;END=351911;LEN=6087	1	0	0	0	0	0	0	0	0	0	0	0	0
347664	<INV>	SVTYPE=INV;END=390365;LEN=42701	0	1	0	0	0	0	0	0	0	0	0	0	0
347664	<INV>	SVTYPE=INV;END=401469;LEN=53805	0	0	0	0	0	0	0	0	0	0	1	1	0
347664	<INV>	SVTYPE=INV;END=436662;LEN=88998	0	0	1	0	0	0	0	0	0	0	0	0	0
357052	<DEL>	SVTYPE=DEL;END=357618;LEN=566	1	0	0	0	0	0	0	0	0	0	0	0	0
362681	<DEL>	SVTYPE=DEL;END=362779;LEN=98	0	0	0	0	0	0	0	0	0	1	0	0	0
373663	<INS>	SVTYPE=INS;END=391064;LEN=101	1	0	0	0	0	0	0	0	0	0	0	0	0
373671	<DUP>	SVTYPE=DUP;END=382660;LEN=8989	0	0	0	0	0	0	0	1	0	0	0	0	0
373671	<INS>	SVTYPE=INS;END=382660;LEN=17353	0	0	0	1	0	0	1	0	0	0	0	0	1
386288	<DEL>	SVTYPE=DEL;END=387303;LEN=1015	0	0	0	0	0	0	0	0	0	1	0	0	0
394229	<INS>	SVTYPE=INS;END=417237;LEN=101	0	1	0	0	0	0	0	0	0	0	0	0	0
401578	<INV>	SVTYPE=INV;END=472283;LEN=70705	0	0	0	0	1	0	1	1	1	0	0	0	0
401578	<INV>	SVTYPE=INV;END=472602;LEN=71024	0	0	0	0	0	0	0	0	0	0	1	1	0
401578	<DEL>	SVTYPE=DEL;END=472283;LEN=70705	0	0	0	0	0	0	0	0	0	1	0	0	0
406108	<INS>	SVTYPE=INS;END=473323;LEN=101	1	0	0	0	0	0	0	0	0	0	0	0	0
407177	<INV>	SVTYPE=INV;END=469893;LEN=62716	0	0	0	1	0	0	0	0	0	0	0	0	0
421176	<INS>	SVTYPE=INS;END=474028;LEN=101	0	1	0	0	0	0	0	0	0	0	0	0	0
439771	<INV>	SVTYPE=INV;END=472602;LEN=32831	0	0	1	0	0	0	0	0	0	0	0	0	0
479157	<INV>	SVTYPE=INV;END=514520;LEN=35363	0	0	0	0	0	0	0	0	0	0	0	1	0

Supplementary Table 6. The Illumina short reads of 184 accessions in citrus used in this study.

Samples	Accessions	Classification	SRR ID	Source
Atalantia_CDSJ	CDSJ	Atalantia	SRR3989910	Wang et al. 2017
Atalantia_GDMM	GDMM	Atalantia	SRR3990142	Wang et al. 2017
Atalantia_HDGKZ	HDGKZ	Atalantia	SRR3990145	Wang et al. 2017
Atalantia_HKC	HKC	Atalantia	SRR3988729	Wang et al. 2017
Atalantia_JBL	JBL	Atalantia	SRR3988460	Wang et al. 2017
Atalantia_SND	SND	Atalantia	SRR3990714	Wang et al. 2017
Atalantia_WNNL	WNNL	Atalantia	SRR3990759	Wang et al. 2017
Atalantia_WNSMW	WNSMW	Atalantia	SRR3992564	Wang et al. 2017
Atalantia_WSD	WSD	Atalantia	SRR3992888	Wang et al. 2017
citron_JY28	JY28	Citron	SRR3948093	Wang et al. 2017
citron_JY4	JY4	Citron	SRR3944125	Wang et al. 2017
citron_JY5	JY5	Citron	SRR3944139	Wang et al. 2017
citron_XZ1	XZ1	Citron	SRR3938253	Wang et al. 2017
citron_XZ	XZ	Citron	SRR3938056	Wang et al. 2017
Climent2013	Climent2013	Mandarin	SRR1022654	Wu et al. 2014
grapefruit_14J	14J	Grapefruit	SRR3926757	Wang et al. 2017
grapefruit_Flame	Flame	Grapefruit	SRR3927405	Wang et al. 2017
grapefruit_HJ	HJ	Grapefruit	SRR9128709	Liang et al. 2020
grapefruit_PAR	PAR	Grapefruit	SRR6188447	Wu et al. 2018
grapefruit_Ruby	Ruby	Grapefruit	SRR3927447	Wang et al. 2017
ichang_JF	JF	Papeda	SRR3929760	Wang et al. 2017
ichang_KM	KM	Papeda	SRR3929763	Wang et al. 2017
ichang_TK	TK	Papeda	SRR3929810	Wang et al. 2017
ichang_XJC	XJC	Papeda	SRR3928212	Wang et al. 2017
ichang_YCC	YCC	Papeda	SRR3928564	Wang et al. 2017
ichang_YCLS	YCLS	Papeda	SRR3929790	Wang et al. 2017
ichang_YCYJ	YCYJ	Papeda	SRR3929943	Wang et al. 2017
ichang_YL	YL	Papeda	SRR3930078	Wang et al. 2017
ichang_ZY	ZY	Papeda	SRR3931949	Wang et al. 2017
JgA12	A12	Kumquat	SRR14766309	PRJNA736109
JgA14	A14	Kumquat	SRR14766314	PRJNA736109
JinLanYou	JLY	pummelo	SRR18120052	PRJNA807745
JSYA	JSY	pummelo	SRR18120051	PRJNA807745
lemon_05L-06	05L-06	Lemon	SRR9129152	Liang et al. 2020
lemon_BJ	BJ	Lemon	SRR14765191	PRJNA736194
lemon_JY22	JY22	Lemon	SRR3948190	Wang et al. 2017
lemon_LS	LS	Lemon	SRR3948277	Wang et al. 2017
lemon_ML	ML	Lemon	SRR3948324	Wang et al. 2017
Ma21CAR	CAR	Shikinari-mikan	SRR14460013	Wu et al. 2021
Ma21CI0	CI0	Citron	SRR14460012	Wu et al. 2021
Ma21CI1	CI1	Citron	SRR14460011	Wu et al. 2021
Ma21CI2	CI2	pummelo x Citron	SRR14460010	Wu et al. 2021
Ma21ISH	ISH	Mandarin	SRR14453878	Wu et al. 2021
Ma21OBN	OBN	Mandarin	SRR14453873	Wu et al. 2021
Ma21R00	R00	Deedee (Nakijin)	SRR14509908	Wu et al. 2021
Ma21RK3	RK3	Mandarin	SRR14453874	Wu et al. 2021
Ma21TK1	TK1	Mandarin	SRR14453879	Wu et al. 2021
mandarin_18H	18H	Mandarin	SRR3749605	Xu et al. 2013
mandarin_19P	19P	Mandarin	SRR3747617	Xu et al. 2013
mandarin_20H	20H	Mandarin	SRR3747635	Wang et al. 2018
mandarin_BTJ	BTJ	Mandarin	SRR3756893	Wu et al. 2014
mandarin_CSNJ	CSNJ	Mandarin	SRR3747609	Wang et al. 2018
mandarin_CYY	CYY	Mandarin	SRR3747399	Wang et al. 2018
mandarin_CZG	CZG	Mandarin	SRR3747583	Wang et al. 2018
mandarin_DFZS	DFZS	Mandarin	SRR5807899	Wang et al. 2018

mandarin_DX1	DX1	Mandarin	SRR5796819	Wang et al. 2018
mandarin_DX2	DX2	Mandarin	SRR5796821	Wang et al. 2018
mandarin_DX3	DX3	Mandarin	SRR5796820	Wang et al. 2018
mandarin_DX4	DX4	Mandarin	SRR5796645	Wang et al. 2018
mandarin_HPJ	HPJ	Mandarin	SRR3750611	Wang et al. 2018
mandarin_HZ	HZ	Mandarin	SRR3747527	Wang et al. 2018
mandarin_JGA	JGA	Mandarin	SRR5796822	Wang et al. 2018
mandarin_JYY	JYY	Mandarin	SRR5796862	Wang et al. 2018
mandarin_KSH	KSH	Mandarin	SRR6188456	Wu et al. 2018
mandarin_KYM	KYM	Mandarin	SRR3820643	Wang et al. 2017
mandarin_LYJ	LYJ	Mandarin	SRR3756887	Wu et al. 2014
mandarin_MLTJ	MLTJ	Mandarin	SRR3750679	Wang et al. 2018
mandarin_MS1	MS1	Mandarin	SRR5796818	Wang et al. 2018
mandarin_MS2	MS2	Mandarin	SRR5796635	Wang et al. 2018
mandarin_MSJ	MSJ	Mandarin	SRR3751832	Wang et al. 2018
mandarin_NFJ	NFJ	Mandarin	SRR5796630	Xu et al. 2013
mandarin_NJ	NJ	Mandarin	SRR3750668	Wang et al. 2018
mandarin_QH117	QH117	Mandarin	SRR3822244	Wang et al. 2017
mandarin_QTJ	QTJ	Mandarin	SRR5796863	Wang et al. 2018
mandarin_S6	S6	Mandarin	SRR10163366	Liang et al. 2020
mandarin_S8	S8	Mandarin	SRR10163365	Liang et al. 2020
mandarin_SCM	SCM	Mandarin	SRR6188448	Wu et al. 2018
mandarin_SJ	SJ	Mandarin	SRR3747529	Wang et al. 2018
mandarin_SNK	SNK	Mandarin	SRR6188455	Wu et al. 2018
mandarin_SPG	SPG	Mandarin	SRR3747540	Wang et al. 2018
mandarin_STJ	STJ	Mandarin	SRR3756933	Wang et al. 2018
mandarin_WHPG	WHPG	Mandarin	SRR5796644	Wang et al. 2018
mandarin_YJNJ	YJNJ	Mandarin	SRR5796865	Wang et al. 2018
mandarin_YSJ	YSJ	Mandarin	SRR3750648	Wang et al. 2018
mandarin_ZHJ	ZHJ	Mandarin	SRR5796927	Wang et al. 2018
N18BUD	BUD	Citron	SRR6188453	Wu et al. 2018
N18CAL	CAL	Calamondin	SRR6188463	Wu et al. 2018
N18CLP	CLP	Mandarin	SRR6188441	Wu et al. 2018
N18COR	COR	Citron	SRR6188458	Wu et al. 2018
N18CSM	CSM	Mandarin	SRR6188440	Wu et al. 2018
N18DNC	DNC	Mandarin	SRR6188439	Wu et al. 2018
N18FOR	FOR	Kumquat	SRR6188462	Wu et al. 2018
N18HUM	HUM	Citron	SRR6188451	Wu et al. 2018
N18ICH	ICH	Papeda	SRR6188454	Wu et al. 2018
N18LIM	LIM	Eureka Lemon	SRR6188464	Wu et al. 2018
N18LMA	LMA	Rangpur lime	SRR6188467	Wu et al. 2018
N18PON	PON	Poncirus	SRR6188465	Wu et al. 2018
N18RRL	RRL	Red Rough lemon	SRR6188444	Wu et al. 2018
N18SourO	SourO	Sour orange	SRR1023728	Wu et al. 2018
N18SVR	SVR	Atalantia	SRR6188460	Wu et al. 2018
N18SweetO	SweetO	Sweet orange	SRR1023639	Wu et al. 2018
N18UNS	UNS	Mandarin	SRR6188446	Wu et al. 2018
N18VEU	VEU	Citron	SRR6188459	Wu et al. 2018
O21CCLYP2	CCLYP2	Poncirus	SRR12323706	PRJNA648176
O21CCNERO	CCNERO	Poncirus	SRR7121817	PRJNA438407
O21JGLYP1	JGLYP1	Poncirus	SRR12323705	PRJNA648176
O21ZKDPI50	ZKDPI50	Poncirus	SRR12323703	PRJNA648176
O21ZKFLY	ZKFLY	Poncirus	SRR12323700	PRJNA648176
O21ZKFMZ	ZKFMZ	Poncirus	SRR12323698	PRJNA648176
O21ZKLileaf	ZKLileaf	Poncirus	SRR12323702	PRJNA648176
O21ZKRUB	ZKRUB	Poncirus	SRR12323699	PRJNA648176
Pt229	Pomeroy	Poncirus	SRR5128229	Wu et al. 2018
Pt234	Flying_dragon	Poncirus	SRR5128234	Wu et al. 2018

PtZK7	ZK7	Poncirus	PRJNA554539	Huang et al. 2021
PtZK8	ZK8	Poncirus	SRR14739657	Huang et al. 2021
pummelo_10Z	10Z	Pummelo	SRR3823645	Wang et al. 2017
pummelo_28H	28H	Pummelo	SRR3823225	Wang et al. 2017
pummelo_AJH	AJH	Pummelo	SRR5802532	Wang et al. 2018
pummelo_CQ-016	CQ-016	Pummelo	SRR3822303	Wang et al. 2017
pummelo_GXY	GXY	Pummelo	SRR5802549	Wang et al. 2018
pummelo_GY-1	GY-1	Pummelo	SRR14765190	PRJNA736194
pummelo_HB	HB	Pummelo	SRR9127779	Liang et al. 2020
pummelo_HHSWY	HHSWY	Pummelo	SRR5802582	Wang et al. 2018
pummelo_NJYPS	NJYPS	Pummelo	SRR3848607	Wang et al. 2017
pummelo_Q-04	Q-04	Pummelo	SRR3823455	Wang et al. 2017
pummelo_RL-06	RL-06	Pummelo	SRR3823409	Wang et al. 2017
pummelo_SMST	SMST	Pummelo	SRR9127778	Liang et al. 2020
pummelo_SR3-2	SR3-2	Pummelo	SRR3822290	Wang et al. 2017
pummelo_STY	STY	Pummelo	SRR14765189	PRJNA736194
pummelo_WSY	WSY	Pummelo	SRR5796633	Xu et al. 2013
pummelo_YNMD	YNMD	Pummelo	SRR9127777	Liang et al. 2020
pummelo_YNSJ	YNSJ	Pummelo	SRR9127776	Liang et al. 2020
sjg21J1	sjg21J1	Kumquat	SRR14766306	PRJNA736109
sjg21K1	sjg21K1	Kumquat	SRR14766305	PRJNA736109
sjg21N1	sjg21N1	Kumquat	SRR14766303	PRJNA736109
sjg21O1-1	sjg21O1-1	Kumquat	SRR14766302	PRJNA736109
sjg_BLS07	sjg_BLS07	Kumquat	SRR14761148	PRJNA735863
sjg_BZ01	sjg_BZ01	Kumquat	SRR14761147	PRJNA735863
sjg_DR01	sjg_DR01	Kumquat	SRR14761143	PRJNA735863
sjg_DYS002-5	sjg_DYS002-5	Kumquat	SRR14761142	PRJNA735863
sjg_FC01	sjg_FC01	Kumquat	SRR14761140	PRJNA735863
sjg_GHS01	sjg_GHS01	Kumquat	SRR14761135	PRJNA735863
sjg_GT01	sjg_GT01	Kumquat	SRR14761134	PRJNA735863
sjg_GZ01	sjg_GZ01	Kumquat	SRR14761133	PRJNA735863
sjg_HK02	sjg_HK02	Kumquat	SRR14761132	PRJNA735863
sjg_HS03	sjg_HS03	Kumquat	SRR14761131	PRJNA735863
sjg_JK09	sjg_JK09	Kumquat	SRR14761130	PRJNA735863
sjg_LS4	sjg_LS4	Kumquat	SRR14761127	PRJNA735863
sjg_LS	sjg_LS	Kumquat	SRR14761128	PRJNA735863
sjg_LT01	sjg_LT01	Kumquat	SRR14761126	PRJNA735863
sjg_MJS02	sjg_MJS02	Kumquat	SRR14761124	PRJNA735863
sjg_MP12	sjg_MP12	Kumquat	SRR14761123	PRJNA735863
sjg_NQ03	sjg_NQ03	Kumquat	SRR14761122	PRJNA735863
sjg_PN01	sjg_PN01	Kumquat	SRR14761121	PRJNA735863
sjg_PN03	sjg_PN03	Kumquat	SRR14761120	PRJNA735863
sjg_RYS	sjg_RYS	Kumquat	SRR14761117	PRJNA735863
sjg_SD01	sjg_SD01	Kumquat	SRR14761116	PRJNA735863
sjg_SK03	sjg_SK03	Kumquat	SRR14761114	PRJNA735863
sjg_SL01	sjg_SL01	Kumquat	SRR14761113	PRJNA735863
sjg_SY02	sjg_SY02	Kumquat	SRR14761111	PRJNA735863
sjg_TX01	sjg_TX01	Kumquat	SRR14761110	PRJNA735863
sjg_TZ	sjg_TZ	Kumquat	SRR14761109	PRJNA735863
sjg_WH	sjg_WH	Kumquat	SRR14761108	PRJNA735863
sjg_WP	sjg_WP	Kumquat	SRR14761107	PRJNA735863
sjg_ZL01	sjg_ZL01	Kumquat	SRR14761104	PRJNA735863
sour_orange_DD	DD	Sour orange	SRR3885049	Wang et al. 2017
sour_orange_GC	GC	Sour orange	SRR14765188	PRJNA736194
sour_orange_GP	GP	Sour orange	SRR9127856	Liang et al. 2020
sour_orange_HZL	HZL	Sour orange	SRR9127851	Liang et al. 2020
sour_orange_JJSC	JJSC	Sour orange	SRR9127843	Liang et al. 2020
sour_orange_KYC	KYC	Sour orange	SRR9127852	Liang et al. 2020

sour_orange_XGCC	XGCC	Sour orange	SRR9127850	Liang et al. 2020
sour_orange_XGTC	XGTC	Sour orange	SRR9127841	Liang et al. 2020
sour_orange_XHC	XHC	Sour orange	SRR9127848	Liang et al. 2020
sour_orange_ZGSC	ZGSC	Sour orange	SRR3916939	Wang et al. 2017
sweet_orange_29B	29B	Sweet orange	SRR3926732	Wang et al. 2017
sweet_orange_A20	A20	Sweet orange	SRR3884831	Wang et al. 2017
sweet_orange_HML	HML	Sweet orange	SRR3883647	Wang et al. 2017
sweet_orange_JC	JC	Sweet orange	SRR3884491	Wang et al. 2017
sweet_orange_LQ	LQ	Sweet orange	SRR3884773	Wang et al. 2017
sweet_orange_NHE	NHE	Sweet orange	SRR3927459	Wang et al. 2017
sweet_orange_SO3	SO3	Sweet orange	SRR5799051	Wang et al. 2017
sweet_orange_WSO	WSO	Sweet orange	SRR4240447	Wang et al. 2017
sweet_orange_XSO	XSO	Sweet orange	SRR4237671	Wang et al. 2017

References:

1. Xu, Q, et al. (2013) The draft genome of sweet orange (*Citrus sinensis*). *Nature Genetics* 45(1):59–66 .
2. Wu GA, et al. (2014) Sequencing of diverse mandarin, pummelo and orange genomes reveals complex history of admixture during citrus domestication. *Nature Biotechnology* 32(7):656-662.
3. Wang X, et al. (2017) Genomic analyses of primitive, wild and cultivated citrus provide insights into asexual reproduction. *Nature Genetics* 49(5):765-772.
4. Wu GA, et al. (2018) Genomics of the origin and evolution of *Citrus*. *Nature* 554(7692):311-316.
5. Liang M, et al. (2020) Evolution of self-compatibility by a mutant Sm-RNase in citrus. *Nature Plants* 6(2):131-142.
6. Wu GA, et al. (2021) Diversification of mandarin citrus by hybrid speciation and apomixis. *Nature Communications* 12(1):4377.

Supplementary Table 7. The identified SVs by 184 short reads mapping.

Position (bp)	Types	End (bp)	Length (bp)
5376	<INV>	END=354410	349034
17075	<DEL>	END=17114	39
41962	<INV>	END=270852	228890
61131	<INV>	END=435483	374352
70665	<INV>	END=415505	344840
70679	<INV>	END=415493	344814
74861	<INV>	END=118391	43530
87613	<DEL>	END=87659	46
95398	<DEL>	END=95437	39
97615	<DEL>	END=97718	103
99663	<DEL>	END=99700	37
100122	<DEL>	END=101386	1264
106573	<INV>	END=219403	112830
111199	<INV>	END=469141	357942
112830	<INV>	END=114004	1174
115323	<INV>	END=292403	177080
148601	<INV>	END=327614	179013
150661	<INV>	END=496990	346329
168554	<INV>	END=274509	105955
169920	<INV>	END=281668	111748
219164	<INV>	END=256671	37507
238454	<INV>	END=390534	152080
243220	<DEL>	END=244021	801
291362	<INV>	END=296756	5394
298165	<INV>	END=444339	146174
322861	<INV>	END=409003	86142
327967	<DEL>	END=328004	37
343390	<DEL>	END=343487	97
343561	<INV>	END=437464	93903
354156	<DEL>	END=354266	110
358061	<DEL>	END=358363	302
359806	<INV>	END=391431	31625
361724	<DUP>	END=393255	31531
377768	<DEL>	END=378789	1021
395376	<DEL>	END=395425	49
402682	<INV>	END=470500	67818
412089	<DEL>	END=412128	39
412664	<INV>	END=506607	93943

Supplementary Table 8. The samples of mandarin in domestication.

Name	Classification_based on nuclear	Classification_based on mitochondria
Climent2013	hybrids	domestication
Ma21ISH	unclassified	wild
Ma21OBN	unclassified	domestication
Ma21RK3	unclassified	wild
Ma21TK1	unclassified	wild
N18CLP	unclassified	wild
N18CSM	unclassified	domestication
N18DNC	unclassified	domestication
N18LMA	unclassified	unclassified
N18RRL	unclassified	unclassified
N18UNS	unclassified	domestication
O21CCLYP2	hybrids	domestication
O21CCNERO	hybrids	domestication
mandarin_18H	MD1	domestication
mandarin_19P	MD2	domestication
mandarin_20H	MD1	domestication
mandarin_BTJ	MD2	domestication
mandarin_CSNJ	MD1	domestication
mandarin_CYY	wild	wild
mandarin_CZG	MD2	domestication
mandarin_DFZS	hybrids	domestication
mandarin_DX1	MD2	domestication
mandarin_DX2	wild	wild
mandarin_DX3	wild	wild
mandarin_DX4	wild	wild
mandarin_HPJ	MD2	domestication
mandarin_HZ	wild	wild
mandarin_JGA	MD2	domestication
mandarin_JYY	wild	wild
mandarin_KSH	unclassified	domestication
mandarin_KYM	hybrids	domestication
mandarin_LYJ	MD2	domestication
mandarin_MLTJ	MD2	domestication
mandarin_MS1	wild	wild
mandarin_MS2	wild	wild
mandarin_MSJ	MD2	domestication
mandarin_NFJ	MD1	domestication
mandarin_NJ	MD2	domestication
mandarin_QH117	hybrids	domestication
mandarin_QTJ	MD2	domestication
mandarin_S6	MD2	domestication
mandarin_S8	MD2	domestication
mandarin_SCM	unclassified	wild
mandarin_SJ	MD2	domestication
mandarin_SNK	unclassified	wild
mandarin_SPG	wild	wild

mandarin_STJ	MD2	domestication
mandarin_WHPG	MD2	domestication
mandarin_YJNJ	MD1	domestication
mandarin_YSJ	MD2	domestication
mandarin_ZHJ	MD1	domestication
sweet_orange_A20	hybrids	domestication

References:
1. Wang L, et al. (2021) Somatic variations led to the selection of acidic and acidless orange cultivars. *Nature Plants* 7(7):954-965.
2. Wu, G.A, et al. (2021) Diversification of mandarin citrus by hybrid speciation and apomixis. *Nature Communication.* 12(1):4377.

Supplementary Table 9. Annotation of the candidate genes in admixture mapping analysis.

GeneID	Pfam_annotation	Swissprot_annotation	P_adj
Fh1g02250	Repeat domain in Vibrio, Colwellia, Bradyrhizobium and Shewanella	Unknown	7E-19
Fh1g04410	Sulfotransferase family	Unknown	2E-75
Fh1g04420	Patatin-like phospholipase	Patatin-like protein 3	NA
Fh1g04430	Patatin-like phospholipase	Patatin-like protein 3	NA
Fh1g04440	CTLH/CRA C-terminal to LisH motif domain	--	0.0096
Fh1g04960	Kinesin motor domain	Kinesin-like protein KIN-4A	1E-15
Fh1g04990	Protein kinase domain	Probable inactive receptor kinase At5g67200	1E-62
Fh1g19290	Protein tyrosine and serine/threonine kinase	Probable receptor-like protein kinase At2g23200	0.0444
Fh1g19300	Unknown	Unknown	3E-20
Fh1g19310	NUDIX domain	Nudix hydrolase 3	0.0013
Fh1g21950	RNA recognition motif. (a.k.a. RRM, RBD, or RNP domain)	U2 small nuclear ribonucleoprotein B	2E-27
Fh1g21960	Enoyl-(Acyl carrier protein) reductase	Short-chain dehydrogenase reductase 2a	2E-78
Fh1g21970	Retrotransposon gag protein	Gag-pol polyprotein	NA
Fh1g22380	Secretory pathway protein Sec39	MAG2-interacting protein 2	0.7377
Fh1g22690	RNase H-like domain found in reverse transcriptase	Genome polyprotein	NA
Fh1g22700	Unknown	Unknown	NA
Fh1g24240	RING-variant domain	Unknown	NA
Fh1g24250	Unknown	Unknown	2E-21
Fh1g24850	DNA polymerase family B	DNA polymerase delta catalytic subunit	2E-89
Fh1g24860	Copine	E3 ubiquitin-protein ligase RGLG3	9E-39
Fh1g24870	2OG-Fe(II) oxygenase superfamily	Gibberellin 20 oxidase 2	NA
Fh1g24880	2OG-Fe(II) oxygenase superfamily	Gibberellin 20 oxidase 1-B	NA
Fh1g28730	Unknown	Unknown	NA
Fh1g28740	Unknown	Unknown	NA
Fh1g29320	Unknown	Unknown	NA
Fh1g29330	NB-ARC domain	Disease resistance RPP8-like protein 3	NA
Fh1g29580	Leucine Rich repeats (2 copies)	Probable inactive receptor kinase At5g10020	1E-86
Fh1g29590	mTERF	Transcription termination factor MTERF8	0.672
Fh1g29860	Domain of unknown function (DUF4220)	Unknown	0.0578
Fh1g29870	Domain of unknown function (DUF4220)	Unknown	7E-05
Fh1g29880	Gamma-glutamyltranspeptidase	Glutathione hydrolase 1	1E-17
Fh1g29950	Unknown	Unknown	5E-15
Fh1g29960	RNA recognition motif. (a.k.a. RRM, RBD, or RNP domain)	UBP1-associated protein 2B	3E-14
Fh2g06720	EamA-like transporter family	WAT1-related protein At5g40240	4E-12
Fh2g06730	PDZ domain	Protease Do-like 9	0.9835
Fh2g06740	EamA-like transporter family	WAT1-related protein At3g28050	0.3384
Fh2g06750	EamA-like transporter family	WAT1-related protein At5g40240	4E-11
Fh2g08140	GDSL-like Lipase/Acylhydrolase	GDSL esterase/lipase At5g14450	6E-242
Fh2g08150	Reverse transcriptase (RNA-dependent DNA polymerase)	LINE-1 retrotransposable element ORF2 protein	2E-16
Fh2g08160	GDSL-like Lipase/Acylhydrolase	GDSL esterase/lipase At5g14450	1E-64
Fh2g08170	Surfeit locus protein 2 (SURF2)	Unknown	2E-18
Fh2g08180	MATH domain	Unknown	NA
Fh2g08310	Sieve element occlusion N-terminus	Protein SIEVE ELEMENT OCCLUSION B	1E-27
Fh2g08320	Mitochondrial domain of unknown function (DUF1713)	Unknown	2E-09
Fh2g08330	Serine aminopeptidase, S33	Alpha/beta hydrolase domain-containing protein 17C	2E-15
Fh2g08540	Unknown	Signaling peptide TAXIMIN 2	2E-30
Fh2g08550	DnaJ C terminal domain	DnaJ homolog subfamily B member 1	0.0005

Fh2g09060	bZIP transcription factor	Basic leucine zipper 61	2E-70
Fh2g09070	Unknown	Glutamate receptor 2.5	3E-38
Fh2g09080	Ligand-gated ion channel	Glutamate receptor 3.2	3E-86
Fh2g09090	Unknown	Unknown	4E-07
Fh2g11140	MULE transposase domain	Protein FAR1-RELATED SEQUENCE 5	NA
Fh2g11150	Translocon-associated protein beta (TRAPB)	Translocon-associated protein subunit beta	0.5238
Fh2g11620	Reverse transcriptase (RNA-dependent DNA polymerase)	Retrovirus-related Pol polyprotein from transposon RE1	NA
Fh2g14240	Reverse transcriptase (RNA-dependent DNA polymerase)	Retrovirus-related Pol polyprotein from transposon TNT 1-94	NA
Fh2g14250	Unknown	Unknown	NA
Fh2g14260	Respiratory-chain NADH dehydrogenase, 30 Kd subunit	NAD(P)H-quinone oxidoreductase subunit J, chloroplastic	0.0046
Fh2g16160	Unknown	Unknown	NA
Fh2g20990	Unknown	Unknown	0.09
Fh2g23780	Vacuolar protein 14 C-terminal Fig4p binding	Protein VAC14 homolog	0.0003
Fh2g23790	Ankyrin repeats (3 copies)	Ankyrin repeat-containing protein At2g01680	0.2119
Fh2g23800	EF hand	Probable calcium-binding protein CML25	7E-206
Fh2g32240	2OG-Fe(II) oxygenase superfamily	Probable prolyl 4-hydroxylase 3	1E-05
Fh2g32250	Unknown	Unknown	NA
Fh2g32260	Unknown	Unknown	2E-28
Fh2g32270	Zinc finger, C3HC4 type (RING finger)	E3 ubiquitin-protein ligase RMA1H1	3E-11
Fh3g08560	Unknown	Alpha-galactosidase 3	1E-23
Fh3g08570	Protein kinase domain	MDIS1-interacting receptor like kinase 2	8E-13
Fh3g10420	Unknown	Unknown	NA
Fh3g18740	mttA/Hcf106 family	Sec-independent protein translocase protein TATA	6E-30
Fh3g18750	PPR repeat	Pentatricopeptide repeat-containing protein At3g18970	1E-16
Fh3g18760	Basic leucine-zipper C terminal	Light-inducible protein CPRF2	1E-65
Fh3g20730	Exportin 1-like protein	Protein HASTY 1	9E-12
Fh3g32850	TCP family transcription factor	Transcription factor TCP23	9E-94
Fh3g32860	Alkaline and neutral invertase	Alkaline/neutral invertase CINV2	3E-55
Fh4g04320	WD domain, G-beta repeat	Protein JINGUBANG	NA
Fh4g04330	Ankyrin repeats (3 copies)	Ankyrin repeat-containing protein ITN1	2E-26
Fh4g04340	Unknown	Unknown	NA
Fh4g04350	Ankyrin repeats (3 copies)	Ankyrin repeat-containing protein ITN1	0.3868
Fh4g04870	Protein kinase domain	Receptor-like protein kinase HSL1	9E-16
Fh4g04880	Poly(A) polymerase central domain	Nuclear poly(A) polymerase 4	0.0193
Fh4g04890	Uncharacterized protein family UPF0054	Endoribonuclease YBEY, chloroplastic	1E-39
Fh4g04900	Unknown	Endoribonuclease YBEY, chloroplastic	2E-20
Fh4g07370	Protein of unknown function, DUF538	Unknown	2E-11
Fh4g07380	Heavy-metal-associated domain	Protein SODIUM POTASSIUM ROOT DEFECTIVE 1	0.9433
Fh4g08400	U-box domain	Putative E3 ubiquitin-protein ligase LIN-1	8E-33
Fh4g08410	Mitochondrial import receptor subunit Tom22	Transcription factor bHLH68	5E-11
Fh4g08960	Unknown	Unknown	3E-05
Fh4g08970	RNA dependent RNA polymerase	Probable RNA-dependent RNA polymerase 3	3E-113
Fh4g10850	Unknown	Unknown	NA
Fh4g10870	Oligosaccharyltransferase subunit 5	Transmembrane protein 258	0.0039
Fh4g14920	Unknown	Unknown	5E-29
Fh4g14930	Unknown	Unknown	NA
Fh4g15070	Unknown	Unknown	NA
Fh4g20530	WD domain, G-beta repeat	Polycomb group protein FIE1	7E-41
Fh4g20540	Unknown	Unknown	0.0123
Fh4g20550	PPR repeat family	Pentatricopeptide repeat-containing protein At4g04790	6E-53

Fh4g20560	Uncharacterised protein family (UPF0242) N-terminus	Unknown	NA
Fh4g20570	Reverse transcriptase-like	Unknown	NA
Fh4g29310	Subtilase family	Subtilisin-like protease SBT2.6	3E-39
Fh4g29320	Glutaredoxin	Glutaredoxin-C4	4E-36
Fh5g22260	gag-polypeptide of LTR copia-type	Unknown	NA
Fh5g22270	Leucine rich repeat	Receptor like protein 27	NA
Fh5g22280	YCF9	Photosystem II reaction center protein Z	0.1573
Fh5g22290	Photosystem II protein	Photosystem II CP43 reaction center protein	0.0381
Fh5g22300	hAT family C-terminal dimerisation region	Zinc finger BED domain-containing protein RICESLEEPER 1	NA
Fh5g24310	O-methyltransferase domain	Anthranilate N-methyltransferase	0.5058
Fh5g45460	Telomere stability C-terminal	Replication stress response regulator SDE2	2E-30
Fh5g45470	Apg6 BARA domain	Beclin-1-like protein	5E-05
Fh5g45480	Protease inhibitor/seed storage/LTP family	Probable non-specific lipid-transfer protein 2	5E-39
Fh5g45490	Protease inhibitor/seed storage/LTP family	Probable non-specific lipid-transfer protein 2	3E-09
Fh5g45500	Ion transport protein	Cyclic nucleotide-gated ion channel 1	0.2674
Fh6g11060	Tetratricopeptide repeat	Unknown	4E-40
Fh6g11070	Unknown	Light-harvesting complex-like protein OHP1	1E-55
Fh6g11080	Cyclin, N-terminal domain	Putative cyclin-D7-1	NA
Fh6g11090	Vacuolar import and degradation protein	Glucose-induced degradation protein 4 homolog	5E-14
Fh6g11100	Legume lectin domain	L-type lectin-domain containing receptor kinase IV.1	6E-64
Fh6g11110	Potato inhibitor I family	Subtilisin inhibitor 1	3E-108
Fh6g11120	Legume lectin domain	L-type lectin-domain containing receptor kinase S.4	5E-15
Fh6g11290	Enoyl-(Acyl carrier protein) reductase	Tropinone reductase homolog	5E-06
Fh6g11300	ATP synthase subunit C	ATP synthase subunit c, chloroplastic	0.3488
Fh6g11310	Amino acid kinase family	Delta-1-pyrroline-5-carboxylate synthase	1E-19
Fh6g16200	Lecithin retinol acyltransferase	Unknown	0.9265
Fh6g16210	Unknown	Unknown	8E-19
Fh6g16220	Unknown	Uncharacterized protein At1g65710	0.6012
Fh6g16230	Unknown	--	9E-17
Fh7g05930	RNase H-like domain found in reverse transcriptase	Transposon Ty3-I Gag-Pol polyprotein	NA
Fh7g05940	Thioredoxin	Protein disulfide isomerase-like 1-3	6E-40
Fh7g05950	Unknown	WPP domain-associated protein (Fragment)	0.0576
Fh7g05960	Serine aminopeptidase, S33	Caffeoylshikimate esterase	5E-14
Fh7g05970	Unknown	Unknown	1E-12
Fh7g06800	Protein of unknown function (DUF4050)	Unknown	0.482
Fh7g06810	GDSL-like Lipase/Acylhydrolase	GDSL esterase/lipase At2g30310	NA
Fh7g06820	Papain family cysteine protease	Probable cysteine protease RD19D	2E-99
Fh7g06830	ACT domain	ACT domain-containing protein ACR10	9E-24
Fh7g08540	Unknown	IQ domain-containing protein IQM3	NA
Fh7g08550	PPR repeat family	Pentatricopeptide repeat-containing protein At2g27610	4E-23
Fh7g08560	Heavy-metal-associated domain	Copper transport protein ATX1	5E-18
Fh7g09040	Sugar (and other) transporter	Inositol transporter 1	2E-15
Fh7g12180	Photosynthetic reaction centre protein	Photosystem II protein D1	0.9035
Fh7g14980	Transferase family	Malonyl-CoA:anthocyanidin 5-O-glucoside-6	NA
Fh7g14990	Unknown	Phenolic glucoside malonyltransferase 1	NA
Fh7g16030	BadF/BadG/BcrA/BcrD ATPase family	N-acetyl-D-glucosamine kinase	9E-21
Fh8g06160	PPR repeat family	Pentatricopeptide repeat-containing protein At2g15630	0.7838
Fh8g06170	CSL zinc finger	Diphthamide biosynthesis protein 3	8E-24

Fh8g06180	Phosphatidylinositol 3- and 4-kinase	Serine/threonine-protein kinase SMG1	1E-13
Fh8g21510	Leucine rich repeat	Protein phosphatase 1 regulatory subunit 7	NA
Fh8g21520	Leucine rich repeat	Receptor-like protein EIX2	4E-21
Fh8g21530	Glycosyl hydrolases family 28	Exopolygalacturonase (Fragment)	NA
Fh9g03310	EF-hand domain pair	Probable serine/threonine-protein phosphatase 2A regulatory subunit B	0.6445
Fh9g03320	Protein tyrosine and serine/threonine kinase	Probable receptor-like protein kinase At5g38990	5E-111
Fh9g03330	GTP1/OBG	GTP-binding protein OBGC, chloroplastic	4E-10
Fh9g14100	Methyltransferase domain	eEF1A lysine and N-terminal methyltransferase	7E-52
Fh9g14110	Potato inhibitor I family	Glu S.griseus protease inhibitor	NA
Fh9g14120	Potato inhibitor I family	Proteinase inhibitor 1	NA
Fh9g14940	Tetratricopeptide repeat	Outer envelope protein 61	8E-20
Fh9g14950	Retrotransposon gag protein	Unknown	NA
Fh9g17180	non-SMC mitotic condensation complex subunit 1	Condensin complex subunit 1	5E-23
Fh9g24810	alpha/beta hydrolase fold	Carboxylesterase 1	1E-17
Fh9g24820	alpha/beta hydrolase fold	Carboxylesterase 1	3E-33
Fh9g24830	alpha/beta hydrolase fold	Carboxylesterase 1	1E-07
Fh9g24840	alpha/beta hydrolase fold	Carboxylesterase 1	3E-09
Fh9g24860	Unknown	Carboxylesterase 1	NA
Fh9g24870	alpha/beta hydrolase fold	Carboxylesterase 1	1E-35
Fh9g25790	AMP-binding enzyme	Oxalate--CoA ligase	5E-48
Fh9g25800	Chlorophyll A-B binding protein	Chlorophyll a-b binding protein 7, chloroplastic	5E-06
Fh9g25810	Sec63 Brl domain	DExH-box ATP-dependent RNA helicase DExH12	NA
Fh9g25820	Sec63 Brl domain	DExH-box ATP-dependent RNA helicase DExH12	NA

Notes:

1. The orange bars indicate significanctly expressed genes between eight pummelos and four mandarins during anther development.
2. The grey band indicate PPR genes related to mitochondrial function.
3. A *P*-value of 'NA' indicates the count of expression < 20.
4. RNA-seq data (cDNA libaraies) obtained from the SRR list: SRR9593690, SRR9593691, SRR9593704, SRR9593696, SRR9593697, SRR9593699, SRR10168370, SRR10168371, SRR8862737, SRR8862738, SRR8862888, SRR8862889, SRR8863081, SRR8863082, SRR8863197, SRR8863198, SRR8868188, SRR8868189, SRR8872464, SRR8872465, SRR8873602, SRR8873603, SRR9124567, SRR9124568, SRR6489420, SRR6489421, SRR6489422, SRR6489423, SRR6489424, SRR6489425.